Published online 27 September 2022

NAR Cancer, 2022, Vol. 4, No. 3 **1**
https://doi.org/10.1093/narcan/zcac027

SFPQ promotes RAS-mutant cancer cell growth by modulating 5′-UTR mediated translational control of CK1α

Venetia Jing Tong Kok[1,†], Jia Ying Tang[1], Gracie Wee Ling Eng[1], Shin Yi Tan[1], Joseph Tin Foong Chin[1], Chun Hian Quek[6], Wei Xuan Lai[4], Teck Kwang Lim[5], Qingsong Lin[5], John Jia En Chua[4,7,8,*] and Jit Kong Cheong[1,2,3,*,†]

[1]Precision Medicine Translational Research Programme, Yong Loo Lin School of Medicine (YLLSoM), National University of Singapore, Singapore, [2]NUS Centre for Cancer Research, National University of Singapore, Singapore, [3]Department of Biochemistry, YLLSoM, National University of Singapore, Singapore, [4]Department of Physiology, YLLSoM, National University of Singapore, Singapore, [5]Department of Biological Sciences, Faculty of Science, National University of Singapore, Singapore, [6]School of Applied Science, Temasek Polytechnic, Singapore, [7]LSI Neurobiology Programme, National University of Singapore, Singapore and [8]Healthy Longevity Translational Research Programme, YLLSoM, National University of Singapore, Singapore

Received January 26, 2022; Revised August 31, 2022; Editorial Decision September 01, 2022; Accepted September 07, 2022

ABSTRACT

Oncogenic mutations in the RAS family of small GTPases are commonly found in human cancers and they promote tumorigenesis by altering gene expression networks. We previously demonstrated that Casein Kinase 1α (CK1α), a member of the CK1 family of serine/threonine kinases, is post-transcriptionally upregulated by oncogenic RAS signaling. Here, we report that the CK1α mRNA contains an exceptionally long 5′-untranslated region (UTR) harbouring several translational control elements, implicating its involvement in translational regulation. We demonstrate that the CK1α 5′-UTR functions as an IRES element in HCT-116 colon cancer cells to promote cap-independent translation. Using tobramycin-affinity RNA-pulldown assays coupled with identification via mass spectrometry, we identified several CK1α 5′-UTR-binding proteins, including SFPQ. We show that RNA interference targeting SFPQ reduced CK1α protein abundance and partially blocked RAS-mutant colon cancer cell growth. Importantly, transcript and protein levels of SFPQ and other CK1α 5′-UTR-associated RNA-binding proteins (RBPs) are found to be elevated in early stages of RAS-mutant cancers, including colorectal and lung adenocarcinoma. Taken together, our study uncovers a previously unappreciated role of RBPs in promoting RAS-mutant cancer cell growth and their potential to serve as promising biomarkers as well as tractable therapeutic targets in cancers driven by oncogenic RAS.

GRAPHICAL ABSTRACT

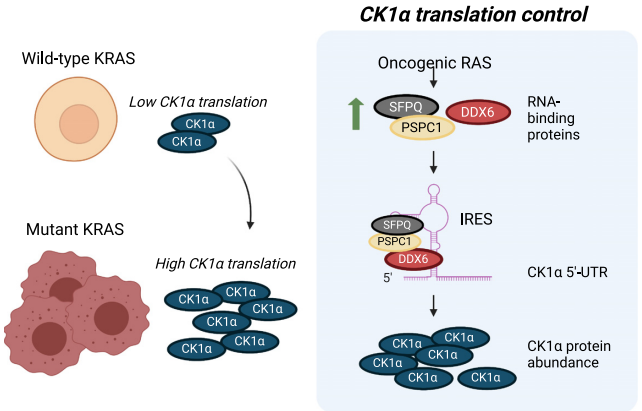

INTRODUCTION

The *RAS* family of small GTPases is one of the most important drivers of human cancer of diverse origins, in part due to the frequent occurrence of activating mutations of *RAS* that confer its oncogenicity. Oncogenic *KRAS,* the most frequently mutated *RAS* isoform, is present in ∼25% of all human cancers (1,2), including >50% of colorectal carcinomas (3). Mutation at codon 12, 13 or 61 locks

*To whom correspondence should be addressed. Tel: +65 66016388; Email: bchcjk@nus.edu.sg
Correspondence may also be addressed to John Jia En Chua. Email: phsjcje@nus.edu.sg
†The authors wish it to be known that, in their opinion, the first and last authors should be regarded as Joint First Authors.

KRAS in a constitutively active state and drives oncogenic progression (4). While KRAS G12V and G12D mutations have the greatest transforming potential (5), studies have revealed tissue-specific codon usage that confers differing prognosis of various therapies. Notably, a recent study in advanced colorectal cancer showed prognostic significance of G13D, but not G12D mutations, in patients treated with cetuximab-based therapy (6,7).

Given that RAS proteins mediate a myriad of signaling networks that include cellular proliferation and survival, it is of little surprise that activating mutations in *RAS* lead to deregulation of these intricate pathways. Although the association between oncogenic KRAS and cancer has been extensively studied, mutant KRAS remains largely undruggable (8). Like many others who have focused on targeting downstream pathways of oncogenic RAS signaling (9,10), we have previously shown that the combined blockade of mutant RAS-induced Casein Kinase 1α (CK1α) alongside lysosomal function is efficacious against RAS-mutant cancer cell growth (11). While CK1α, a serine/threonine protein kinase, is known as an effector of cellular processes such as Wnt/β-Catenin signaling, NF-κB signaling, cell cycle progression and autophagy (12), less is known about its role(s) and regulation in RAS signaling.

We previously demonstrated that the increase in CK1α protein abundance is mediated via the PI3K/AKT/mTOR effector pathway of oncogenic RAS signaling (11). Notably, the elevated CK1α protein abundance observed in KRAS mutant cells was not accompanied by a corresponding increase in its mRNA transcript level (11,12), indicating that CK1α expression may be controlled by post-transcriptional or translational mechanisms. In recent years, increasing evidence has shown that post-transcriptional mechanisms involving 5′ and 3′ untranslated regions (UTRs) regulate translational efficiency (13). The UTRs function through an interplay between the primary sequence and structural motifs that are collectively termed *cis*-regulatory elements. *Cis*-regulatory elements present in 5′-UTRs include upstream open reading frame (uORF), internal ribosome entry site (IRES), G-quadruplexes and others. In addition, *trans*-acting factors such as RNA-binding proteins (RBP) and IRES *trans*-acting factors (ITAF) bind to some of these *cis*-regulatory elements to modulate complex transcript modifications and/or translation processes, including mRNA export, mRNA stabilization and translation initiation (13,14). Given the extensive evidence of 5′-UTR deregulation in human diseases and its propensity to regulate gene expression in a highly specific manner (13,15), we hypothesized that the regulation of CK1α in RAS-mutant cancer cells may involve these 5′-UTR-specific elements and their associated RBPs.

Via *in silico* analysis, we showed that the 5′-UTR of CK1α is exceptionally long (588 nucleotides) and GC-rich (67%) as compared to other 5′-UTRs of the CK1 family. We demonstrate that it is a strong repressor of translation in a cell-free system. In the cellular context, however, we observed significant de-repression of translation, suggesting that *trans*-acting cellular factors interact with the 5′-UTR of CK1α to modulate translation efficiency. We further performed tobramycin aptamer-mediated RNA pull-down assays using full length CK1α 5′-UTR, followed by mass spectrometry and identified proteins that bind specifically to the 5′-UTR of CK1α transcript to modulate its protein expression. Among the identified RBPs, we demonstrate that SFPQ, SRSF4, DDX6, Moesin and PSPC1 are expressed in a mutant KRAS-specific manner in HCT-116 colon cancer cells. We further showed that depletion of SFPQ downregulated CK1α protein expression and partially blocked the proliferation of RAS-mutant cancer cells of diverse tissue origins. Notably, ectopic expression of CK1α rescued the SFPQ depletion-induced cell loss, suggesting that CK1α is a critical effector downstream of SFPQ.

MATERIALS AND METHODS

Plasmid constructs and cell lines

The bipromoter vector psiCHECK™-2 was purchased from Promega (C8021) and the bicistronic vector pR_F was a kind gift from Dr Luísa Romão (16). The psiCHECK™-2 vector carries *Renilla* luciferase (RLuc) and firefly luciferase (FLuc) under two independent promoters (Figure 2D). All primer sequences used to generate the CK1α 5′-UTR truncation mutants are listed in Supplementary Table S10. More details can be found in Supplementary Methods. Other plasmid constructs used in this study include pCMV-Myc (Clontech, 631604), pCMV-Myc-PSF wildtype (Addgene, #35183), pCMV-Myc-PSFΔRRM1 (Addgene, #35376), pCMV-Myc-PSFΔRRM2 (Addgene, #35377), pcDNA3.1-CK1α wildtype-3HA and pcDNA3.1-CK1α kinase-dead (K46A)-3HA. Creation and use of the CK1α plasmid constructs have been previously described in (11). Details of human cell lines used and their culture conditions can be found in Supplementary Methods.

5′ Rapid amplification of cDNA ends (5′ RACE)

5′ RACE analysis of RNA isolated from HCT-116 KRAS (WT/G13D) cells was carried out using a 5′/3′ RACE kit (2nd Generation, Roche, 03-353-621-001), according to manufacturer's protocol. Details can be found in Supplementary Methods.

In silico analysis of CK1α 5′-UTR

The nucleotide sequence of CK1α 5′-UTR was analysed using *cis*-regulatory element and secondary structure prediction algorithms, respectively. These include NetStart (https://services.healthtech.dtu.dk/service.php?NetStart-1.0), IRESite (http://iresite.org), QGRS Mapper (https://bioinformatics.ramapo.edu/QGRS/index.php) and Mfold (http://www.unafold.org). Phylogenetic analysis was generated by the Clustal Omega multiple sequence alignment program (https://www.ebi.ac.uk/Tools/msa/clustalo/). Details can be found in Supplementary Methods.

Cell-free in-vitro transcription and translation

Monocistronic construct was generated by digesting the CK1α 5′-UTR psiCHECK™-2 constructs with restriction enzyme AfeI (NEB, R0652S) in CutSmart® buffer for 1 h at 37°C. Following which, *in-vitro* transcription was performed with T7 Ribomax™ Express Large Scale RNA Production Systems (Promega, P1320) for 45 min at 37°C.

DNA template was removed by incubating with 1 U/μg RQ1 RNase-Free DNase for 15 min at 37°C, followed by RNA isolation using the RNeasy Mini Kit (QIAGEN, 74106). RNA samples were normalized to 2 μg prior to *in vitro* translation using the Rabbit Reticulocyte Lysate System (Promega, L4960) in accordance with manufacturer's protocol. Luciferase activity was measured using the *Renilla* Luciferase Assay System (Promega, E2810).

Plasmid transfection and luciferase assays

Cells were seeded 24 h prior to transfection. Transfection was performed with jetPRIME® transfection reagent (Polyplus transfection, 101000001). Samples were lysed with 1× Passive Lysis Buffer (Promega, E1941), supplemented with 1 x complete Protease Inhibitor (Roche, 11697498001). The Dual-Luciferase® Assay System (Promega, E1980) was used to measure both *Renilla* and firefly luminescence. For bipromoter (psiCHECK™-2) assays, *Renilla* luminescence was normalized to firefly luminescence, using firefly luminescence to control for varying transfection efficiencies. For the bicistronic reporter assay, IRES activity was determined by normalizing firefly luminescence to *Renilla* luminescence (17).

Tobramycin RNA-pulldown assay

The RNA-pulldown protocol was modified from a previously published protocol (18). Details can be found in Supplementary Methods. List of buffers used in the Tobramycin RNA-pulldown assay can be found in Supplementary Table S11.

Coomassie blue staining, mass spectrometry (MS) and data analysis

Protein eluates from the tobramycin RNA pulldown assay were resolved on 10% sodium dodecyl sulfate-polyacrylamide gel electrophoresis (SDS-PAGE) gel, followed by Coomassie blue staining overnight. Protein bands were visualised using ChemiDoc System (Bio-Rad), and the bands at the 75 kDa and 40 kDa regions were excised and sent for mass spectrometry analysis by NUS Protein and Proteomics centre (PPC). Further details can be found in Supplementary Methods.

RNA-immunoprecipitation (RIP) assay

HCT-116 (WT/G13D) colon cancer cells were lysed in modified RIPA buffer (50 mM Tris–HCl, 150 mM NaCl, 0.25% sodium deoxycholate, 1% NP-40, 1 mM EDTA, 0.1% SDS) with 1 x complete Protease Inhibitor (Roche, 11697498001) and 1 mM DTT (Roche). For the RIP, 500 μg of total protein was incubated with 2 μg of anti-Myc/c-Myc antibody (F-7) (Santa Cruz Biotechnology, sc-40) overnight at 4°C. RIP was performed using Pierce™ Protein A/G Magnetic Beads (Thermo Fisher Scientific, 88802) according to the manufacturer's protocol. At the final wash, the RNA/antibody complexes were split into two tubes of equal volumes for elution of protein and RNA. Proteins were eluded by adding 2× SDS-PAGE Sample Buffer and boiling at 95°C for 10 min before subsequent analysis with SDS-PAGE. RNA was eluded with TRIzol™ Reagent (Invitrogen™, 15596026) and chloroform in a ratio of 1:5, followed by RNeasy Mini Kit (QIAGEN, 74106). Extracted RNA was then subjected to quantitative RT-PCR analysis.

In silico analysis of candidate RBP expression in public cancer databases

Transcript and protein expression of SFPQ and other candidate RBPs using the open-access the Cancer Genome Atlas (TCGA) cancer datasets (via Gene Expression Profiling Interactive Analysis; GEPIA) and the National Cancer Institute's Clinical Proteomic Tumor Analysis Consortium (CPTAC) datasets (via UALCAN; http://ualcan.path.uab.edu) respectively. Statistical significance is calculated by Student's *t*-test, considering unequal variance.

Quantitative real-time polymerase chain reaction (qRT-PCR)

First strand cDNA was synthesized using the BlitzAmp cDNA Synthesis kit (MiRXES, 1203101), then analyzed by quantitative PCR using the BlitzAmp qPCR Master Mix (MiRXES, 1204202) and QuantStudio™ 5 Real-Time PCR System (Applied Biosystems). All primer sequences used in semi-quantitative or quantitative PCR are listed in Supplementary Table S9.

Western blot (WB) and antibodies

Details can be found in Supplementary Methods.

RNAi of human SFPQ expression

Cells were transfected with short interfering RNA (siRNA) molecules specifically targeting human SFPQ using either DharmaFECT (Horizon Discovery, T-2001–04) or jetPRIME® transfection reagent (Polyplus transfection, 101000001). Cells were seeded to ∼80% cell density 24 h before actual experiments for optimal transfection efficiency. Transfection was performed with 50 nM of either non-targeting siRNA (siControl; Horizon Discovery D-001810-0X), pooled (ON-TARGETplus SMARTpool) (Horizon Discovery, D-001810–10-20) or individual siRNAs (siSFPQ 06–09; Horizon Discovery, LQ-006455–00-0020) targeting human SFPQ for 24–72 h, as per manufacturer's protocol. The target sequences of the individual siRNAs are as follows: siSFPQ-06 (5′-UGAAAGGGCUGUUGUAAUA -3′), siSFPQ-07 (5′-GAUGUGAUAUUUAGGCUUU-3′), siSFPQ-08 (5′-GAACAAAUGAGGCGCCAAA-3′), siSFPQ-09 (5′-GUACGAAGGCCCAAACAAA -3′).

Clonogenic growth assays

Clonogenic growth assays were performed as previously described (11). Details can be found in Supplementary Methods.

Statistical analysis

All statistical analyses were performed using GraphPad PRISM 9 (GraphPad Software, San Diego, CA, USA), using one sample *t* test, Student's unpaired two-tailed *t* tests set at a 95% confidence level, or one-way ANOVA with Dunnett's multiple comparisons test for direct comparison of experimental group(s) to its control group, or three-way ANOVA with Turkey multiple comparisons test. Data is presented as mean ± standard error of the mean (mean ± SEM). *P* values of <0.05 are considered to be statistically significant.

RESULTS

The 5′-UTR of CK1α contains several putative *cis*-regulatory elements of translation

While studies have shown enhanced CK1α expression in oncogenic RAS signaling (11,19,20), the underlying regulatory mechanisms remain poorly understood. We previously reported that the elevated CK1α protein abundance was not accompanied by a corresponding increase in its mRNA transcript level, indicating that CK1α is likely regulated by post-transcriptional or translational mechanisms (11). The CK1α mRNA sequence retrieved from GenBank® includes a 588-nucleotide(nt) long and 67% Guanine/Cytosine (GC)-rich 5′-UTR (accession number: NM_001025105.2). It is one of the longest 5′-UTR as compared to those from other isoforms of the CK1 family (Figure 1A, Supplementary Table S1). Using a cDNA library prepared from HCT-116 colon cancer cells, we performed 5′ Rapid amplification of cDNA ends (RACE) to amplify the 5′-UTR of CK1α. RACE products were then cloned into pCR™2.1-TOPO™ vector, prior to the evaluation of their sequence length using PCR-DNA gel electrophoresis. We observed that the median length of the amplicons was ∼500-nt (Figure 1B, Supplementary Table S2). However, we cannot rule out that shorter amplicons arose either from complications in amplification as a result of the high GC content of the sequence, or from alternative splicing events in the 5′-UTR. Given these issues, we opted to synthesise the 588-nt long CK1α 5′-UTR based on the deposited GenBank sequence.

The median 5′-UTR length of human messenger RNA (mRNA) transcripts is typically 218-nt long and longer transcripts have a higher probability of harbouring potential translational regulatory elements (21,22). Thus, we examined if the unusually long CK1α 5′-UTR contains *cis*-regulatory elements that could control CK1α protein expression in RAS-mutant cancer cells. *In silico* analyses using NetStart, IRESite and QGRS Mapper predicted that the 588-nt 5′-UTR is densely decorated with *cis*-regulatory elements, including an upstream open reading frame (uORF), internal ribosome entry sites (IRESs) and G-quadruplexes (Figure 1C). NetStart predicted that the uORF at position 193 of the CK1α 5′-UTR is a potential translation start site (Supplementary Tables S3-4). In addition, IRESite identified IRES sequences of various lengths throughout the CK1α 5′-UTR. Notably, the CK1α 5′-UTR aligned with putative IRES sequences of *Gtx, LEF1 and Hsp70* (23–25) at nucleotide positions 233–257, 305–333 and 468–491, respectively (Supplementary Table S5). QGRS Mapper also predicted five G-quadruplexes within the CK1α 5′-UTR with a G-score of >10 (Supplementary Table S6).

Although most members of the CK1 family have 5′-UTRs of substantial length and GC content (Supplementary Table S1), the distribution of predicted *cis*-regulatory elements for protein expression control of CK1α do not appear to be well conserved among the CK1 isoforms (Supplementary Figure S1A and Table S3). Furthermore, alignment of 5′-UTR sequences from all CK1 isoforms using Clustal Omega also uncovered poor conservation between putative *cis*-regulatory elements identified in the CK1α 5′-UTR and those from the other CK1 isoforms (Figure 1D). While the 5′-UTRs of CK1α and CK1γ2 appeared to be more closely related phylogenetically (Figure 1D), the sequence conservation between them remains low (Supplementary Figure S1B, C). Overall, our findings highlight that the *cis*-elements of the CK1α 5′-UTR are unique to the α-isoform and could be responsible for regulating its translation in KRAS-mutant cancers (11).

The 5′-UTR of CK1α is a potent repressor of translation

The linear and structural *cis*-regulatory elements often contribute interdependently to the regulation of translation (13). Apart from its extensive length, the GC-rich CK1α 5′-UTR has a highly negative predicted folding free energy ($\Delta G = -293.4$ kcal/mol), suggesting the presence of stable secondary structures that may affect translation efficiency. Structures with ΔG lower than –35 kcal/mol are known to inhibit translation (26). Notably, with Mfold (27), we identified three prominent secondary structures stemming from the folding of nucleotides from positions 1–88 and 492–588 ($\Delta G = -71.1$ kcal/mol), 228–295 ($\Delta G = -39.0$ kcal/mol) and 350–427 ($\Delta G = -24.0$ kcal/mol) of the CK1α 5′-UTR, respectively. The first two structures are likely to inhibit translation (Figure 2A).

To evaluate whether these putative *cis*-regulatory elements affect translation, we constructed truncation mutants of the CK1α 5′-UTR lacking the *cis*-elements that were predicted to regulate protein expression (Figure 2B). Full-length CK1α 5′-UTR and its truncation mutants were cloned into the psiCHECK™-2 vector, so that the *Renilla* luciferase (RLuc) open reading frame is preceded by these CK1α 5′-UTR variants. Equal amounts of linearized empty or CK1α 5′-UTR-containing psiCHECK™-2 vectors were then used as templates to program cell-free *in vitro* transcription and translation (TNT) assays. Remarkably, we observed that the normalized RLuc activity under the control of full-length CK1α 5′-UTR (FL588nt) was 60-fold lower (0.0165 ± 0.00121) than the empty vector control (Figure 2C), suggesting that full-length 5′-UTR of CK1α confers near-complete suppression of RLuc translation. During the course of these studies, NCBI published a revision to the CK1α 5′-UTR sequence (GenBank® Accession Number NM_001025105.3), where the first 114 nucleotides from the original 588-nt CK1α 5′-UTR were removed. We examined the revised shortened 475-nt 5′-UTR of CK1α (FL475nt) using the same cell-free system and demonstrated that it also dramatically reduced RLuc translation (Figure 2C).

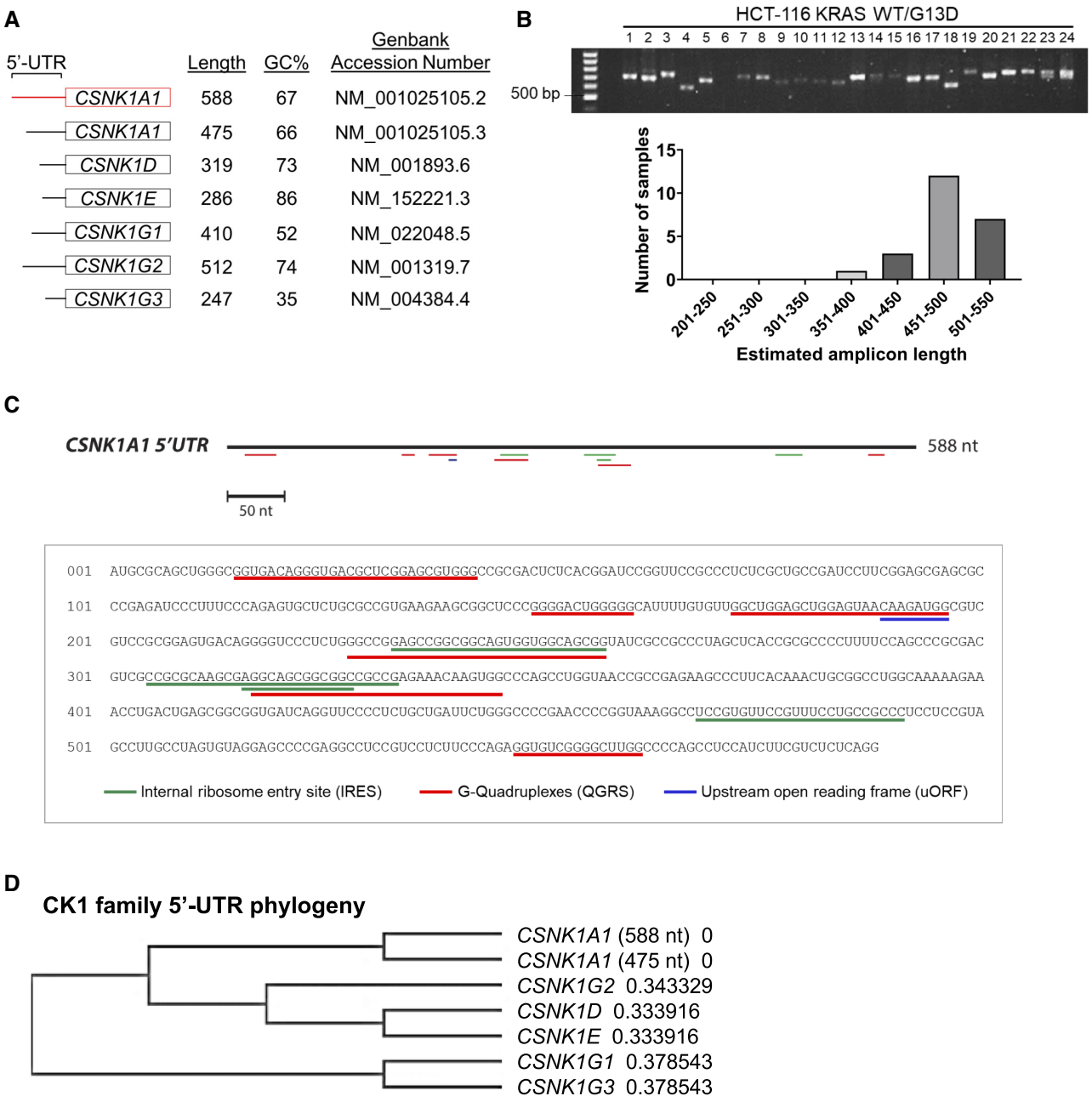

Figure 1. CK1α has a long and structured 5′-UTR consisting of *cis*-regulatory elements unique to its isoform. (**A**) Comparison of the 5′-UTRs of all CK1 isoforms. Length, GC% and corresponding NCBI accession numbers are listed accordingly. The earlier version of CK1α 5′-UTR is included in the analysis (boxed in red). (**B**) 5′-RACE analysis of RNA isolated from HCT-116 KRAS (WT/G13D) cells. 5′-RACE amplicons of CK1α 5′-UTR were subcloned into TOPO-TA vectors and plasmid DNA with 5′RACE amplicons from randomly selected clones were screened by PCR using M13 Forward/Reverse primers. Amplicons were resolved by 1% DNA agarose gel and transcript lengths were estimated by subtracting the multiple cloning site (200 bp) from the size of the visualized bands on the gel. Average transcript length is 500 bp, ranging from 351 bp to 550 bp. (**C**) Graphic representation of putative *cis*-regulatory elements within the CK1α 5′-UTR (NM_001025105.2) identified by NetStart, IRESite and QGRS Mapper. Predicted IRES shown were filtered by >70% identity and *e*-value <10. *In silico* analysis revealed that the 5′-UTR of CK1α contains one upstream open reading frame at position 193 (blue), as well as several G-quadruplexes (red) and IRESs (green). Further details can be found in Supplementary Tables S3–S6. (**D**) Phylogenetic tree generated by Clustal Omega using the 5′-UTR sequences of the CK1 family. The phylogenetic distance is denoted next to the corresponding gene. NCBI accession numbers of sequences used are listed in (A).

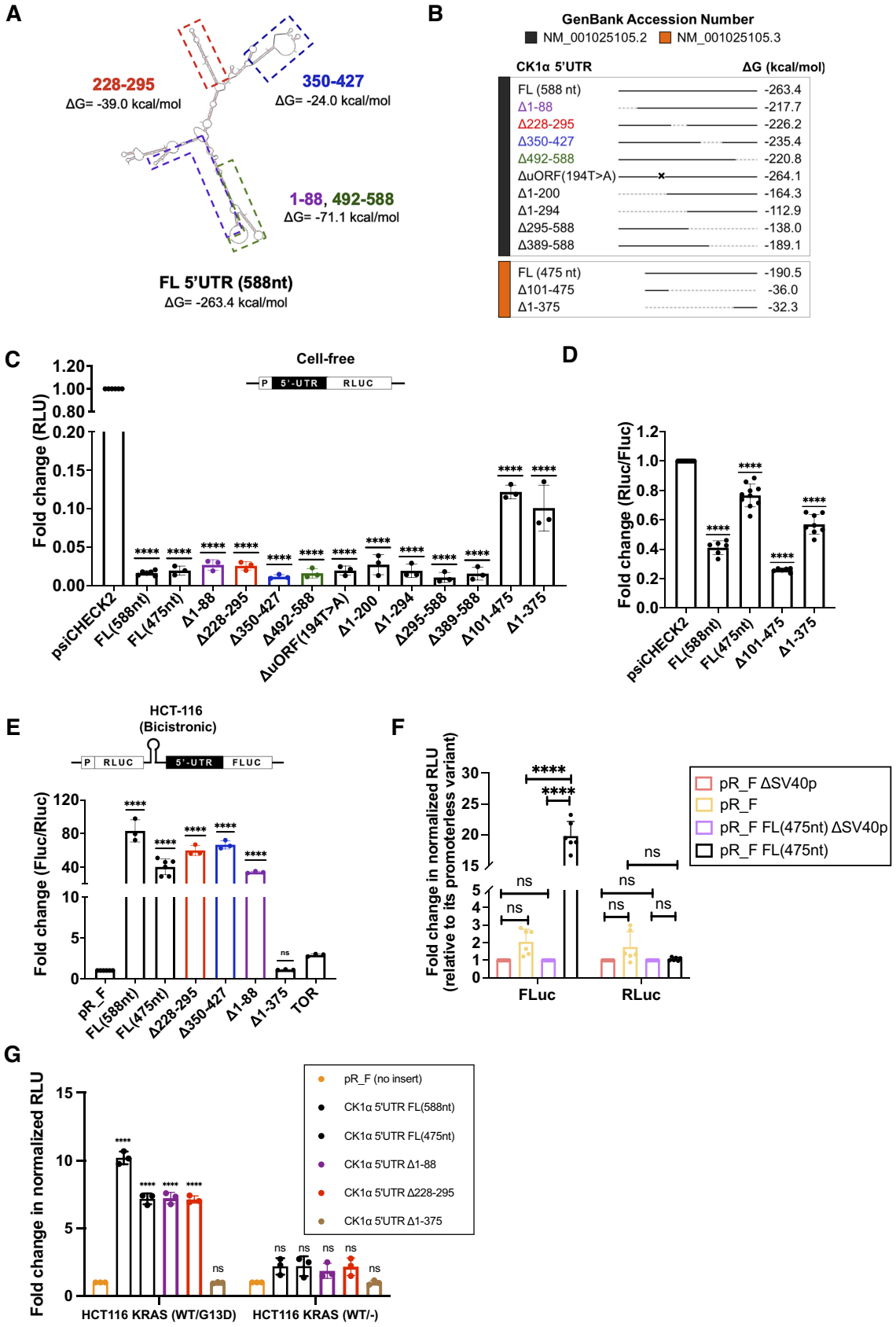

Figure 2. The 5′-UTR of CK1α modulates translation. (**A**) Mfold prediction of the full-length 5′-UTR and individual RNA structures that were deleted in the list of mutants in (B), with their corresponding Δ*G* values (27). (**B**) Schematic representation of the CK1α 5′-UTR mutants used in this study. Horizontal

Furthermore, to test whether the Mfold-predicted secondary structures within the CK1α 5′-UTR plays a role in repressing translation, we systematically eliminated these regions via truncation PCR mutagenesis (Supplementary Figure S2A). Intriguingly, elimination of the predicted CK1α 5′-UTR secondary structures (Δ1–88nt, Δ228–295, Δ350–427, Δ492–588), the G-quadruplexes (Δ1–88, Δ228–295, Δ492–588) or the uORF (ΔuORF(194T>A)) had no appreciable effect in reversing the repression of RLuc translation (Figure 2C). Since linear and structural *cis*-regulatory elements work cooperatively to regulate translation (13), we generated CK1α 5′-UTR mutants with broader deletions (Δ1–200, Δ1–294, Δ295–588, Δ389–588, Δ101–475, Δ1–375). While most of these truncation mutants failed to rescue RLuc translation *in vitro*, we demonstrated that the ultra-short 100-nt truncation mutants (Δ101–475, Δ1–375) partially restored RLuc translation. Collectively, the data strongly indicate that near full-length sequence of CK1α 5′-UTR is involved in regulating protein translation *in vitro* (Figure 2C).

Cellular trans-acting factors interact with the CK1α 5′-UTR to modulate translation

Consistent with data from the *in vitro* TNT assays, normalized RLuc activities from full-length CK1α 5′-UTR-containing psiCHECK™-2 vector (bipromoter) remained significantly lower as compared to the empty vector control when these constructs were introduced into HCT-116$^{KRAS\ (WT/G13D)}$ colon cancer cells (Figure 2D). Nevertheless, the extent of translational suppression in the cancer cells was significantly reduced. While the magnitude of translational repression was 60-fold in the cell-free system, only a reduction of 1.3–2.4-fold was observed in cells. These data suggest that, as compared to a cell-free system, the presence of additional factors in a cellular system allows partial relief of translational suppression by the CK1α 5′-UTR. Differential translational properties of the CK1α 5′-UTR FL(588nt) and FL(475nt) could be attributed to the additional upstream start codon present in the former UTR and the large secondary structure formed by its first 150 nucleotides, both of which are absent in the shorter 5′-UTR variant (Figure 2A). Thus, loss of the first 114 nucleotides in CK1α 5′-UTR FL(475nt) removes these inhibitory elements, thereby allowing more translation to occur. Deletion of neither nucleotides 101–475 nor nucleotides 1–375 could restore RLuc translation to the extent observed in CK1α 5′-UTR FL(475nt) (Figure 2D). Deletion of the first 375 nucleotides in the Δ1–375 mutant removed many of the identified elements inhibitory to translation. Moreover, ΔG of the resultant 5′-UTR is only –32.3 kcal/mol, which is easily resolved by the scanning 43S ribosome. However, translation of the Δ1–375 mutant remains appreciably lower than FL(475nt), suggesting that the first 375 nucleotides contained element(s) required for the preferential translation of FL(475nt) in cancer cells.

Stable secondary structures such as those identified in the 5′-UTR of CK1α transcript could either act via recruiting *trans*-acting factors (i.e. RNA binding proteins and their associated co-factors) to regulate translation or, under certain conditions, additionally function as internal ribosome entry sites (IRESs) (28). We first assessed if increased translation in the presence of the CK1α 5′-UTR could be IRES-mediated in HCT-116 cells using the bicistronic dual-luciferase system (pR_F) vector (16). Expression of RLuc and Firefly luciferase (FLuc) reporters from the pR_F vector is driven by a single promoter, with their coding sequences separated by an intercistronic region carrying a stable hairpin structure that prevents spurious translation of FLuc as a result of stop codon read-through by ribosomes (29). Insertion of a functional IRES element, such as the mTOR 5′-UTR, increases FLuc translation despite the presence of the stable hairpin structure. Thus, increased ratio of FLuc/RLuc activity from these constructs over the empty pR_F vector is indicative of putative IRES activity of the inserted 5′-UTR sequence. In this study, the full-length CK1α 5′-UTR, its truncated variants, or the mTOR 5′-UTR was individually cloned into the pR_F vector intercistronic region. We first validated the integrity of the resultant bicistronic transcripts using RT-PCR assays (Sup-

←

black lines and dotted lines represent encoded regions and deleted regions respectively. Point mutation (T→A) is denoted by (x). Δ*G* values of the most stable structure for each mutant are listed on the right. (**C**) Elimination of individual *cis*-regulatory elements failed to restore translation of *Renilla* luciferase in cell-free transcription and translation assays. RLuc activity was measured and first normalized to total RNA input. Fold change represents RLuc normalized to the empty vector (psiCHECK2). All data is represented by mean ± SEM, $n \geq 3$. ****$P < 0.0001$, as tested by one-way ANOVA with Dunnett's multiple comparisons test; ns denotes not statistically significant. (**D**) Schematic representation of the psiCHECK2 reporter plasmid. RLuc: *Renilla* luciferase, FLuc: Firefly luciferase. CK1α 5′-UTR was inserted upstream of RLuc, both RLuc and FLuc have independent promoters. Expression of FL CK1α 5′-UTR (588 nt and 475nt) in mutant KRAS (WT/G13D) increased RLuc protein expression. Data is normalized to vector control (psiCHECK2). All data is represented by mean ± SEM, $n \geq 3$. ****$P < 0.0001$, as tested by one-way ANOVA with Dunnett's multiple comparisons test. (**E**) Schematic representation of the bicistronic reporter plasmid (16). IRES activity is measured as FLuc to RLuc ratio, normalized to the vector control (pR_F). Elimination of putative IRES elements identified in the 5′-UTR only interfered with its IRES activity partially. IRES activity of the CK1α 5′-UTR extends to the first two-thirds of the 5′-UTR. All data is represented by mean ± SEM, $n \geq 3$. *$P < 0.05$, **$P < 0.01$, ***$P < 0.001$, ****$P < 0.0001$, as tested by one-way ANOVA with Dunnett's multiple comparisons test; ns denotes not statistically significant. (**F**) The observed IRES activity is not a result of cryptic promoters in the CK1α 5′-UTR. Luciferase activity in cells transfected with the indicated plasmids was measured and normalized to the amount of plasmids transfected into the cells. Fold change in normalized relative light unit (RLU) for Firefly luciferase (FLuc) and Renilla luciferase (RLuc) was calculated relative to their respective promoterless variant (e.g pR_F/pR_F ΔSV40p and pR_F FL(475nt)/pR_F FL(475nt) ΔSV40p). Three-way ANOVA with Turkey comparison test was performed to determine whether statistical difference between groups is significant. ns: p-value not significant; ****P-value <0.0001. Data was generated from two biological replicates with technical triplicates ($n = 6$). (**G**) FL and mutant CK1α 5′-UTR variants were transfected into HCT-116 cells with or without KRAS G13D mutation. IRES activity is measured as FLuc to RLuc ratio, normalized to the vector control (pR_F). Elimination of putative IRES elements identified in the 5′-UTR only interfered with its IRES activity partially. IRES activity of the CK1α 5′-UTR extends to the first two-thirds of the 5′-UTR. IRES activity of the CK1α 5′-UTR is abolished in HCT-116 cells without mutant KRAS. All data is represented by mean ± SEM, $n = 3$. ****$P < 0.0001$, as tested by one-way ANOVA with Dunnett's multiple comparisons test; ns denotes not statistically significant. RLU: relative light unit.

plementary Figure S2B). Consistent with a previous report, increased FLuc activity was observed when the mTOR 5′-UTR (TOR) was inserted into the intercistronic region (Figure 2E) (16). Remarkably, almost all variants of CK1α 5′-UTR tested (including the 588-nt and 475-nt full-length UTRs as well as Δ228–295, Δ350–427 and Δ1–88) exhibited strong IRES activity of between 20- to 80-fold as compared to the empty bicistronic control vector (Figure 2E). We also found that truncation of the first 375 nt of the CK1α 5′-UTR (Δ1–375), leaving the last 100 nucleotides, was required to abolish its IRES activity. This indicated that a large contiguous segment of the CK1α 5′-UTR constituted the IRES element.

To rule out any potential contribution to FLuc activity from cryptic promoters that may be present in the CK1α 5′-UTR, we generated pR_F and pR_F CK1α 5′-UTR FL (475nt) reporter plasmids (pR_F ΔSV40p and pR_F FL (475nt) ΔSV40p) that lack the SV40 promoter and chimeric intron (Supplementary Figure S2C). We then confirmed that the HCT-116 cells were transfected with comparable amounts of reporter plasmids prior to the dual luciferase reporter assays (Supplementary Figure S2C). Notably, the removal of SV40 promoter from the bicistronic reporter plasmid dramatically reduced both FLuc and RLuc activity to background levels (Supplementary Figure S2D). We found that transfection with the promoterless pR_F FL (475nt) ΔSV40p results in minimal luciferase activity in HCT-116 cells (two biological replicates with technical triplicates), indicating that the observed FLuc expression/activity from pR_F FL (475nt) is likely due to the IRES activity of the CK1α 5′-UTR, and not cryptic promoter activity (Figure 2F). This is similar to the 5′-UTRs of Sterol Regulatory Element Binding Protein 1-alpha (SREBP 1α) (30) and mammalian target of rapamycin (mTOR) (16), which possess IRES activity (without any cryptic promoter activity) to allow cells to bypass adverse conditions and efficiently translate SREBP 1α as well as mTOR to trigger cellular stress responses. In addition, the IRES activity of CK1α 5′-UTR variants (including the 588-nt and 475-nt full-length UTRs as well as Δ1–88, Δ228–295 and Δ1–375) appears to be repressed in HCT-116$^{KRAS\,(WT/-)}$ cells (Figure 2G). Collectively, our data show that the CK1α 5′-UTR can regulate protein translation in colon cancer cells by functioning as an IRES element in a mutant KRAS-specific manner.

RNA-tobramycin pulldown-mass spectrometry assays identify CK1α 5′-UTR-interacting proteins

Cellular IRES-mediated translation in eukaryotes frequently involves RNA-binding proteins (RBPs) or IRES trans-acting factors (ITAFs). To date, only a limited number of cellular ITAFs have been discovered (31). In order to identify proteins that could potentially bind to the CK1α 5′-UTR and function as ITAFs, we *in vitro* transcribed the longest (588 nt) full-length 5′-UTR tagged to a tobramycin aptamer and subsequently used it for RNA-tobramycin pull-down assays (18) against lysates obtained from HCT-116 KRAS (WT/G13D) cells. Following protein resolution on SDS-PAGE and staining, bands differentially visualized between the CK1α 5′-UTR-bait and control (bait-less) pulldowns at 75 and 40 kDa (Figure 3A) were excised and sent for identification by mass spectrometry (see Materials and Methods for details). The complete workflow is illustrated in Figure 3B and Supplementary Figure S3A.

In total, 49 proteins in the 75 kDa band and 153 proteins in the 40 kDa band were specifically identified from pulldowns using the CK1α 5′-UTR bait (Supplementary Figure S3B, Table S7). Metascape analyses showed that the proteins associated with the CK1α 5′-UTR were significantly enriched in RNA-related processes, including RNA metabolism, ribonucleoprotein complex biogenesis, ncRNA metabolism, translation and RNA catabolic processes (Figure 3C). As such, we screened for RNA-binding proteins (RBPs) through the NCBI database. These RBPs were then ranked according to protein content and protein score, before an additional round of filtering using the CRAPome database (Figure 3D) (32) and RPISeq (Supplementary Table S8) (33). Notably, all three components of the *Drosophila* behaviour/human splicing (DBHS) protein family, Splicing factor proline/glutamine rich (SFPQ or PSF), Paraspeckle protein component 1 (PSPC1 or PSP1) and non-POU domain-containing octamer-binding protein (NONO or p54nrb), were identified from pulldowns using the CK1α 5′-UTR (Figure 3D, Supplementary Table S7). Apart from the DBHS proteins, the ERM protein Moesin, RNA helicase DDX6 and proteins of the heterogeneous nuclear ribonucleoprotein (hnRNP) families are also among the top RBP candidates found to be associated with the CK1α 5′-UTR by targeted mass spectrometry. Other noteworthy RBPs that regulate translation and RNA splicing include Serine And Arginine Rich Splicing Factor 4 (SRSF4) and Far Upstream Element-Binding Protein 2 (FUBP2). These RBPs have been previously reported to promote tumorigenesis (34–43). We validated the top RBP candidate from our original CK1α 5′-UTR-tobramycin pulldown assays via immunoblotting and show that SFPQ is indeed present in the CK1α 5′-UTR RNA-pulldown cell lysates and absent in control pulldowns (Figure 3E). Our CK1α 5′-UTR-tobramycin enrichment mass spectrometry approach is specific as we demonstrated, via mass spectrometry (Supplementary Table S7) and Western blot (Supplementary Figure S3C), that the 3′UTR-associated RBP, LARP1 (44), is not enriched the CK1α 5′-UTR RNA-pulldown cell lysates. We also performed RNA immunoprecipitation (RNA-IP) by myc-tagged wild-type and RNA-recognition motif-deficient mutants of SFPQ and determined the presence of CK1α 5′-UTR in the immunoprecipitated complex using targeted quantitative-PCR. We first confirmed that known RNA targets of SFPQ such as DDX23 and hnRNPU are enriched in immunoprecipitated wildtype myc-SFPQ (Supplementary Figure S3D-E) (45). We then observed enrichment of endogenous and ectopically expressed CK1α 5′-UTR in the immunoprecipitated wildtype myc-SFPQ by 24-fold and 108-fold, respectively (Figure 3F). Importantly, elimination of either RNA recognition motif (RRM1 or RRM2) of SFPQ impeded pulldown of the CK1α 5′-UTR, indicating that both RRMs are required for SFPQ to interact with the CK1α 5′-UTR.

To further understand whether specific secondary structures of the CK1α 5′-UTR are critical for its recruitment of SFPQ, full-length (FL) and mutant CK1α 5′-UTR variants [FL(475nt), Δ1–88, Δ228–295 and Δ1–375] were co-

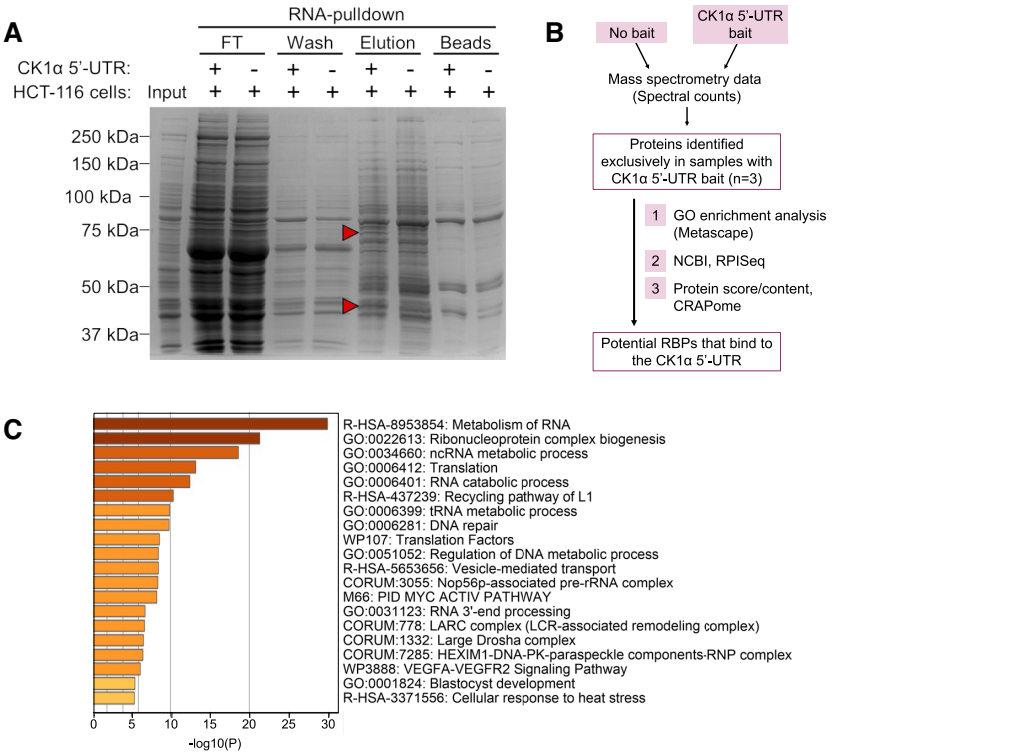

D

Region excised	Accession Code	Protein Identity	Biol. Replicates	Score^	Protein Content (%)#	CRAPome† datasets (Found/Total)
75 kDa	SFPQ_HUMAN	Splicing factor, proline- and glutamine-rich	3	71.33	0.23	201/411
	SRSF4_HUMAN	Serine/arginine-rich splicing factor 4	3	50.33	0.17	131/411
	MOES_HUMAN	Moesin	2	613.50	1.61	78/411
	FUBP2_HUMAN	Far upstream element-binding protein 2	2	77	0.34	133/411
	FUS_HUMAN	RNA-binding protein FUS	2	165	0.19	188/411
	CSDE1_HUMAN	Cold shock domain-containing protein E1	2	65	0.15	67/411
	NPM_HUMAN	Nucleophosmin	2	47	0.15	252/411
40 kDa	PSPC1_HUMAN	Paraspeckle component 1	2	129	0.31	82/411
	DDX6_HUMAN	Probable ATP-dependent RNA helicase DDX6	2	216	0.29	129/411
	HNRPM_HUMAN	Heterogeneous nuclear ribonucleoprotein M	2	196.5	0.21	220/411
	HNRPQ_HUMAN	Heterogeneous nuclear ribonucleoprotein Q	2	67.5	0.15	197/411
	PHF6_HUMAN	PHD finger protein 6	2	38.5	0.07	42/411
	FKBP4_HUMAN	Peptidyl-prolyl cis-trans isomerase FKBP4	2	87.5	0.07	95/411
	ENOA_HUMAN	Alpha-enolase	2	59	0.07	223/411
	NOLC1_HUMAN	Nucleolar and coiled-body phosphoprotein 1	2	38	0.07	120/411
	ERF3A_HUMAN	Eukaryotic peptide chain release factor GTP-binding subunit ERF3A	2	52.5	0.05	59/411

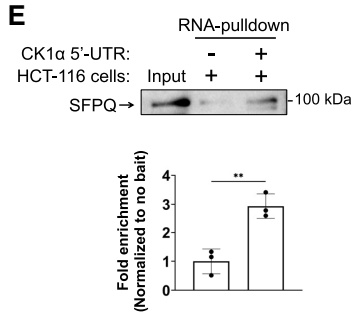

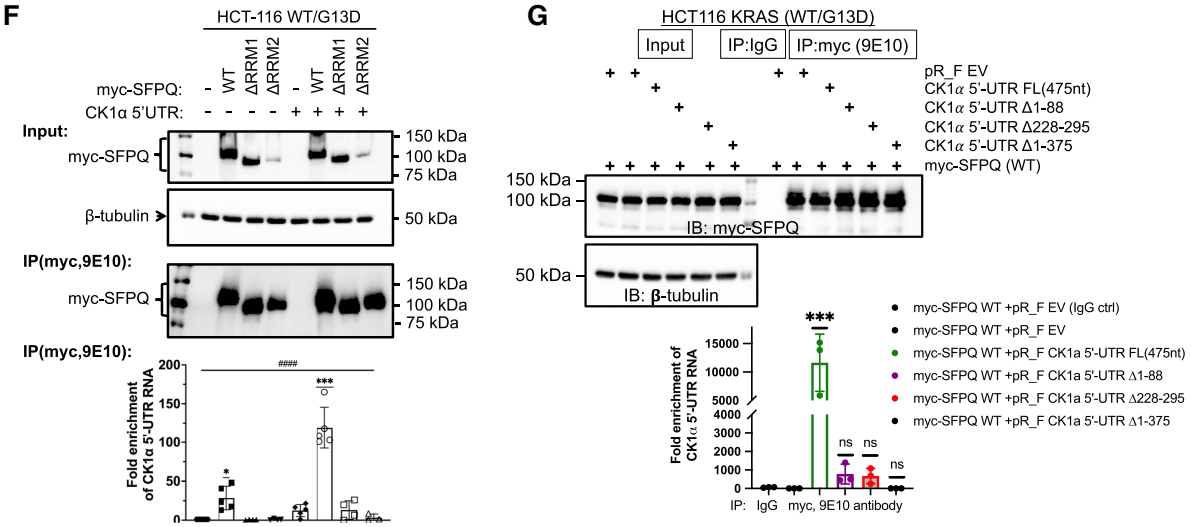

Figure 3. SFPQ and other RNA-binding proteins (RBPs) interact with the CK1α 5′-UTR. (**A**) Identification of unique RBPs of CK1α 5′-UTR RNA using Tobramycin RNA pulldown assays followed by SDS-PAGE and Coomassie Blue staining. Input loaded is 2% of total protein amount used for the

transfected with myc-SFPQ (WT), followed by immunoprecipitation using the myc (9E10) antibody, RNA isolation and RT-qPCR to assess the enrichment of FL and mutant CK1α 5′-UTR variants. While semi-quantitative RT-PCR indicated that the FL and mutant CK1α 5′-UTR variants are expressed in cell lysates used for myc (9E10) antibody-driven immunoprecipitation (Supplementary Figure S3F), we observed that the interaction between myc-SFPQ (WT) and CK1α 5′-UTR was significantly abolished when a subset of stem-loop structures in the CK1α 5′-UTR were eliminated (Δ1–88 and Δ228–295) (Figure 3G). Furthermore, interaction between myc-SFPQ (WT) and CK1α 5′-UTR interaction was completely abolished when more than two-thirds of the CK1α 5′-UTR (Δ1–375) was eliminated. Taken together, multiple stem-loop structures in the CK1α 5′-UTR are critical for its interaction with SFPQ. As deletion of individual secondary structure of CK1α 5′-UTR (Δ1–88 and Δ228–295) did not appear to eliminate its protein translation potential in cells (Figure 2E) but significantly abolished its interaction with SFPQ (Figure 3G), we postulate that other CK1α 5′-UTR-interacting RBPs identified by our mass spectrometry analysis may be recruited to these CK1α 5′-UTR truncated mutants to promote the protein translation.

Transcript and protein levels of CK1α 5′-UTR RBPs are elevated in KRAS-mutant cancers

Given the upregulation of CK1α protein in KRAS-mutant colon cancer cells, we examined if the protein expression of these CK1α-regulating RBPs are also enhanced in a mutant RAS-specific manner. When compared to their isogenic G13D-knockout (WT/-) counterpart, protein levels of SFPQ, SRSF4, DDX6, Moesin and PSPC1 were indeed elevated in the KRAS-mutant (WT/G13D) colon cancer cells (Figure 4A-B, Supplementary Figure S4A). This is consistent with an earlier report that identified RBPs to be downstream components of the Ras/Mitogen-Activated Protein Kinase Signaling Pathway in *Drosophila* (46).

Since activating mutations of KRAS frequently occur in colon and lung cancers (47), we mined publicly available cancer datasets such as TCGA (48) (via Gene Expression Profiling Interactive Analysis of TCGA cancer datasets; GEPIA) (49) and UALCAN (50,51), and performed meta-analysis for evidence of dysregulation of SFPQ in human cancer patients. We additionally included four other CK1α 5′-UTR RBPs (DDX6, SRSF4, Moesin and PSPC1) from our pulldowns in the analyses. Our TCGA analysis revealed upregulation of SFPQ and PSPC1 transcript abundance in a variety of mutant RAS-driven human cancers, including colon adenocarcinoma (COAD), rectal adenocarcinoma (READ), urothelial bladder carcinoma (BLCA), lung adenocarcinoma (LUAD) and lung squamous cell carcinoma (LUSC) (Figure 4C, Supplementary Figure S4B). We also found SRSF4 transcript upregulation in COAD (Supplementary Figure S4C). Notably, we also identified that upregulation of the 5-RBP transcript signature (SFPQ, PSPC1, SRSF4, DDX6 and Moesin) predicts poorer overall survival of patients with colon and lung adenocarcinoma (Supplementary Figure S4D). Furthermore, the UALCAN proteomics data demonstrated that protein levels of SFPQ, DDX6, SRSF4 and PSPC1 are upregulated in human colon and lung tumours when compared to their normal tissue counterparts (Figure 4D–E, Supplementary Figure S4E–J). Notably, protein levels of SFPQ, SRSF4, PSPC1 and DDX6 are elevated as early as stage I in these tumours, suggesting that these RBPs may be useful biomarkers for early detection of human colon and lung cancers.

SFPQ knockdown in HCT-116 cells reduces CK1α protein abundance and suppresses cell growth

Increased expression of CK1α 5′-UTR RBPs in the presence of activating KRAS mutations and association with increased CK1α levels suggest that perturbation of RBPs could be a strategy to curtail cancer cell proliferation. Since SFPQ is the top RBP candidate identified from our mass spectrometry screen, we employed the small interfering RNA (siRNA) strategy to deplete SFPQ in HCT-116 KRAS-mutant colon cancer cells. Abundance of CK1α proteins, but not its transcripts, were indeed reduced when SFPQ expression was downregulated by siRNAs (Supplementary Figure S5A–D). Next, we assessed if targeting SFPQ expression is sufficient to block proliferation of HCT-116 cells and whether such approach is mutant-KRAS specific. We performed a timed study that involved clonogenic growth assays followed by crystal violet staining to measure the effects of SFPQ depletion on the growth rates of

←

pulldown. Protein bands at 75 kDa and 40 kDa regions (indicated by red arrowheads) were excised and sent for mass spectrometry analyses by NUS Protein and Proteomics Centre (PPC), $n = 3$. (**B**) Flowchart of mass spectrometry analysis. Only proteins identified exclusively in samples with CK1α 5′-UTR bait were selected for further evaluation. (**C**) Metascape enrichment analysis of proteins associated with the CK1α 5′-UTR. Bar graph of enriched terms are shown, with a colour scale to represent statistical significance. Darker colour indicates lower *P*-value. (**D**) List of RNA-binding proteins (RBPs) found to be associated with the CK1α 5′-UTR. Proteins are ranked according to number of experiments (or biological replicates) in which the protein was identified, followed by protein content[#] and protein score[^]. RBPs selected for further target validation are shown in red. (**E**) Western blot analysis of RNA-pulldown lysates to validate the interaction of CK1α 5′-UTR with SFPQ. Input loaded is 4% of total protein amount used for pulldown. Fold enrichment is calculated by normalizing to bait-less sample. Data is represented by mean ± SEM, $n = 3$. $^{**}P < 0.01$, as tested by unpaired *t*-test with Welch's correction. (**F**) RNA-immunoprecipitation with myc-SFPQ (WT, ΔRRM1 or ΔRRM2) with or without CK1α 5′-UTR. IP experiments were performed with c-myc (9E10) antibody and analyzed by western blot using anti-SFPQ monoclonal antibody to. Precipitated RNA from the same experiment was analyzed by qRT-PCR with primers amplifying the 5′-UTR. Fold enrichment of RNA relative to pCMV (empty vector control for the myc-SFPQ plasmids) was calculated and normalized to total protein precipitated. All individual data points represent values from independent experiments (with mean ± SEM). Statistical significance was assessed by one sample *t*-test, $^{*}P < 0.05$, $^{**}P < 0.01$, and one-way ANOVA, $^{\#\#\#\#}P < 0.0001$. (**G**) RNA-immunoprecipitation with myc-SFPQ (WT) with full-length or mutant CK1α 5′-UTR [FL(475nt), Δ1–88, Δ228–295 and Δ1–375]. IP experiments were performed with IgG control or c-myc (9E10) antibody and analyzed by western blot using anti-SFPQ monoclonal antibody. Precipitated RNA from the same experiment was analyzed by qRT-PCR with primers amplifying the 5′-UTR. Fold enrichment of RNA relative to pR_F EV (empty vector control for the full-length or mutant CK1α 5′-UTR plasmids) was calculated and normalized to total protein precipitated. All data is represented by mean ± SEM, $n = 3$. $^{****}P < 0.0001$, as tested by one-way ANOVA with Dunnett's multiple comparisons test. ns denotes not statistically significant.

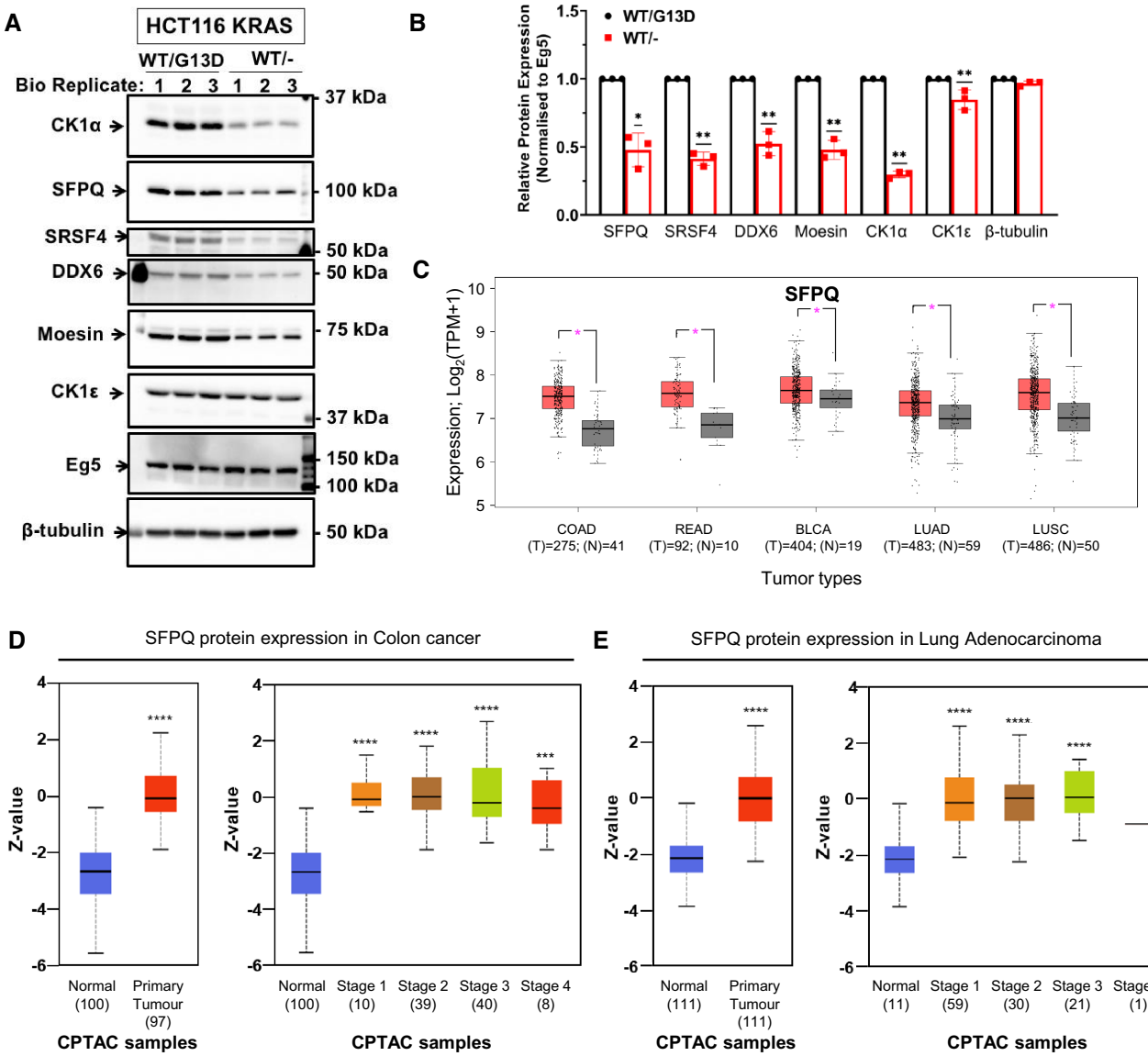

Figure 4. SFPQ and DDX6 are upregulated in human colorectal and lung cancers. (**A**) Western blot analysis of the expression of SFPQ, SRSF4, Moesin and DDX6 in HCT-116 cells with or without KRAS G13D mutation, $n = 3$. (**B**) Image J densitometry analysis of (A), normalized to Eg5 loading control. All individual data points represent values from independent experiments (with mean ± SEM). Statistical significance was assessed by one sample *t*-test, $*P < 0.05$, $**P < 0.01$. (**C**) Comparison of SFPQ expression in tumor (T; red) versus normal (N; grey) tissues using Gene Expression Profiling Interactive Analysis (GEPIA; http://gepia.cancer-pku.cn/) (49). Matched cancer and normal data were extracted from the indicated TCGA datasets and transcript expression [in log2(Transcript per million, TPM, +1)] was analyzed using a *P*-value <0.05 cut-off (denoted by the magenta asterisk). COAD: colon adenocarcinoma; READ: rectal adenocarcinoma; BLCA: urothelial bladder carcinoma; LUAD: lung adenocarcinoma; LUSC: lung squamous cell carcinoma. UALCAN analysis of SFPQ protein expression in (**D**) colon cancer and (**E**) lung adenocarcinoma, where normal tissue is compared to primary tumor, as well as, tumor tissues at various stages, using the CPTAC datasets.

HCT-116$^{KRAS(WT/G13D)}$ and HCT-116$^{KRAS(WT/-)}$ cells. Cells transfected with non-targeting/control siRNA (siControl) or SFPQ-targeting siRNA (siSFPQ-06 or 09) were stained with crystal violet at 24 h, 48 h and 120 h (Figure 5A). SFPQ depletion strongly impaired the growth of HCT-116$^{KRAS(WT/G13D)}$, but not HCT-116$^{KRAS(WT/-)}$, cells (Figure 5A, Supplementary Figure S5D). In particular, time required for siControl, siSFPQ-06 and siSFPQ-09 cells to reach 50% max growth was 64, 108 and 110 hours, respectively (Figure 5A). Similar results were observed in the DLD1 KRAS isogenic colon cancer cell lines (Supplementary Figure S5E, F). We also transfected other RAS-mutant cancer cell lines (PANC-1, A549, T24 and NCI-H1299) with siControl or SFPQ-targeting siRNA (siSFPQ-06 or 09) (Supplementary Figure S5G-J) and stained them with crystal violet at 24, 48 and 120 h. As illustrated in Figure 5B-C and Supplementary Figure S5K-M, SFPQ depletion significantly blocked the growth of these other RAS-mutant cancer cell lines. Notably, SFPQ depletion in RAS-mutant cancer cell lines (HCT-116$^{KRAS(WT/G13D)}$ and A549) also induced PARP cleavage, a hallmark of cell death (Figure 5D).

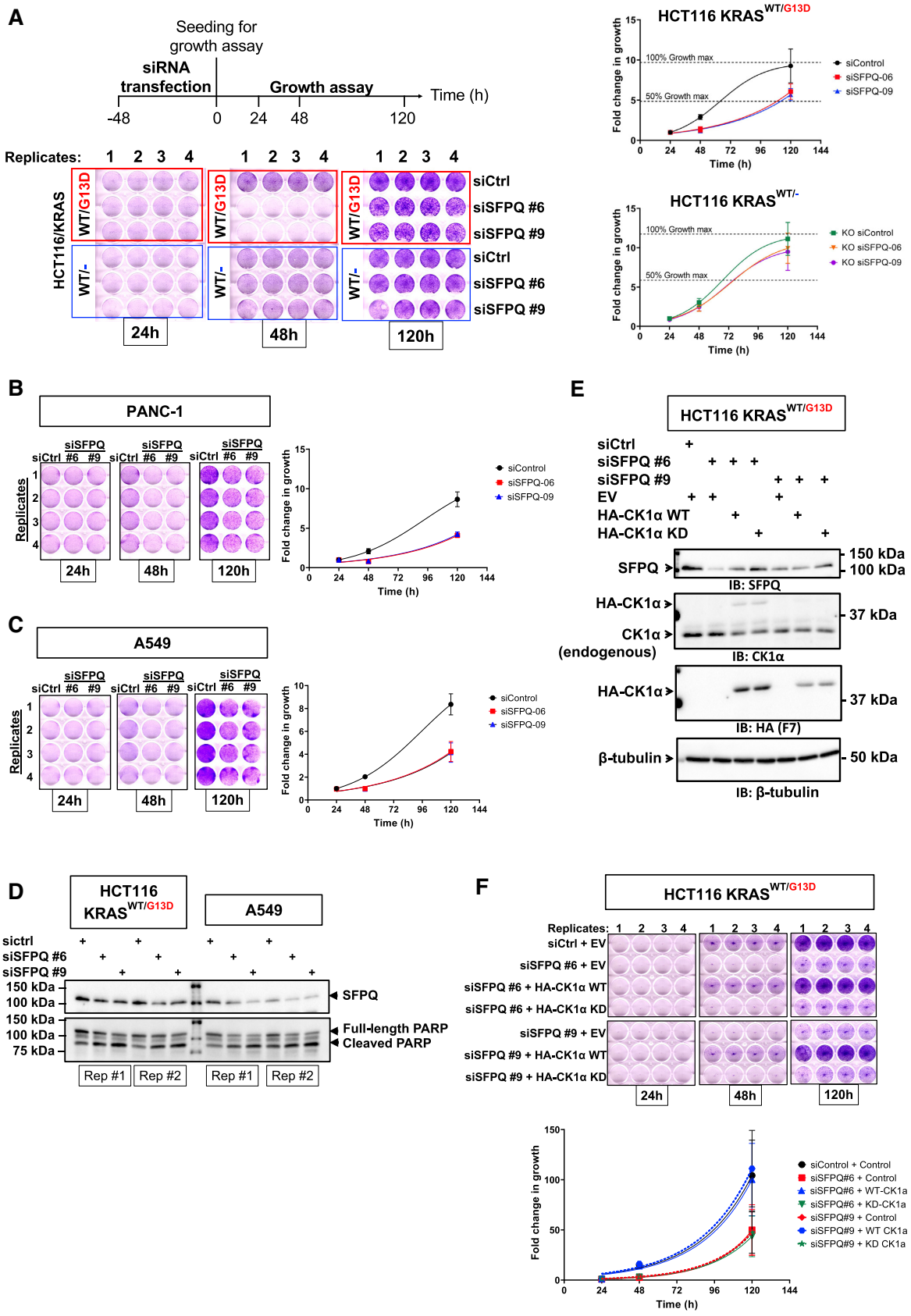

Figure 5. SFPQ is required for KRAS-mutant cancer cell growth. (**A**) SFPQ depletion reduced growth of HCT-116 KRAS-mutant (WT/G13D) cells, but not KRAS-KO (WT/-) cells. Growth assay followed by crystal violet staining of HCT-116 KRAS-mutant (WT/G13D) and KRAS-KO (WT/-) cells

Finally, to further assess whether CK1α is a key effector downstream of SFPQ, we ectopically expressed control vector or vector with HA-tagged CK1α (HA-CK1α) in SFPQ-depleted HCT-116$^{KRAS(WT/G13D)}$ cells (Figure 5E) and measured their growth rates by the crystal violet clonogenic cell growth assays. As shown in Figure 5F, ectopic expression of WT HA-CK1α (WT-CK1α) but not its kinase dead mutant (KD-CK1α) rescued the SFPQ depletion-induced cell loss, suggesting that CK1α is not only a critical effector downstream of SFPQ but its kinase activity is important for the regulation of KRAS-mutant HCT-116 cancer cell growth. Taken together, our findings indicate that targeting the SFPQ-CK1α axis is a viable approach to restrict proliferation of RAS-mutant cancer cells of diverse tissue origins.

DISCUSSION

The CK1 family of serine/threonine kinases forms an independent branch of the human kinome and regulates diverse processes critical to the maintenance of cellular and organismal homeostasis (52). Despite reports of CK1 dysregulation in a myriad of human diseases, the underlying molecular mechanism that governs the expression of CK1 remains largely elusive. We recently showed that protein abundance of the CK1 alpha isoform (CK1α) is specifically upregulated via the PI3K-AKT-mTOR effector pathway, but not its mRNA (11,53). This regulatory mechanism of CK1α abundance in RAS-mutant cancers appears to be distinct from those that have been previously described, including gain-of-function mutation (54) and microRNA (miRNA)-dependent transcript stability (55).

In this study, we show that CK1α protein expression is regulated by post-transcriptional mechanisms involving its 5′-UTR. Transcripts with long 5′-UTRs tend to encode transcription factors, protooncogenes, growth factors/receptors, and their corresponding proteins are typically poorly expressed under normal conditions (56). We found the 5′-UTR of CK1α mRNA to be longer than the average 5′-UTR length across most species (22) and consists of multiple stable secondary structures (Figures 1A and 2A). Although *in silico* analyses predicted a number of *cis*-acting regulatory elements in the 5′-UTR of CK1α (Figure 1C), we demonstrate that its near full-length sequence is required for the control of CK1α protein expression, in part due to its IRES activity (Figure 2C–E). To date, IRESs have been implicated in a growing list of human diseases, including cancer (57–59). As opposed to the canonical 5′ cap-dependent translation, IRESs typically serve as an alternative mode of translation initiation for protein synthesis in cells that have been exposed to unfavourable stress conditions (60). While it remains unknown whether the mRNA of CK1α is 5′ capped, we demonstrate that the presence of IRES in the 5′-UTR is necessary for robust CK1α protein expression and the growth of RAS-mutant cancer cells. This is the first report, to the best of our knowledge, that demonstrate IRES dependency of CK1α protein expression. Future investigation to study the contribution of other CK1α 5′-UTR *cis*-regulatory elements (e.g. G-quadruplexes) to CK1α mRNA translation control is also warranted. For instance, G-quadruplexes in 5′-UTR have been shown to recruit Eukaryotic translation initiation factor 4A (eIF-4A) to promote cap-dependent translation initiation of a number of oncogenes, super enhancer-associated transcription factors, and epigenetic regulators (61). This mode of protein translation initiation is negatively regulated by 4EBP1 downstream of the mTOR pathway (62). Notably, we previously demonstrated that mutant RAS, via its PI3K/AKT/mTOR effector pathway, regulates CK1α protein expression (11). Our mass spectrometry data also identified Eukaryotic translation initiation factor 3G (eIF-3G) to be a CK1α 5′-UTR-interacting protein (Supplementary Table S7). As eIF-3G occupancy in GC-rich 5′-UTR of mRNAs has been recently shown to govern neuronal protein levels to control neuronal activity states (63), we speculate that the predicted G-quadruplexes in the CK1α 5′-UTR may recruit eIF-3G to promote eIF-4F complex (eIF-4E/eIF-4G/eIF-4A)-dependent translation of CK1α mRNA (64).

In the context of cap-independent translation, IRES elements recruit IRES trans-acting factors (ITAFs) to facilitate ribosome assembly at the 5′-UTR. Many ITAFs have been shown to be RBPs with known RRMs and they regulate modifications, stability, transport and translation of RNA in cells (65). Although RBPs have long been found to be integral to the regulation of protein expression and function (66), enrichment of RBPs in human cancers has only been recently reported (67). We postulate that a subset of RBPs may bind to IRESs in the 5′-UTR of CK1α to enhance its translation in a mutant RAS-specific manner. We first isolated endogenous CK1α 5′-UTR-bound proteins using tobramycin-RNA aptamer purification and analyzed the RBPs via targeted mass spectrometry. Notably, all three components of the DBHS protein family (SFPQ, PSPC1 and NONO) were found to be associated with the

←

was performed after treatment with siControl (siCtrl) or siSFPQ (#6 and #9). Timeline of the experiment is illustrated. Following siRNA transfection, the same number of cells were seeded at a low density at 0 h. Cells were stained with crystal violet at the indicated time points (24, 48 and 120 h) to assess for growth rate. 100% Growth max represents maximum growth of cells respective to siCtrl, where cells are at 100% confluence. The assay was performed in quadruplicates and repeated in two other independent experiments, $n = 12$. All individual data points represent values from independent experiments (with mean ± SEM). SFPQ depletion reduced growth of (**B**) PANC-1 and (**C**) A549 cells. Growth assay followed by crystal violet staining of PANC-1 and A549 cells was performed after treatment with siControl (siCtrl) or siSFPQ (#6 and #9), according to the same protocol as above. (**D**) Depletion of SFPQ in RAS-mutant cancer cells induces PARP cleavage. Western blot analysis of siRNA-mediated knockdown of SFPQ [using siSFPQ (#6 and #9)] in HCT-116 KRAS (WT/G13D) and A549 cells was performed by antibodies that target SFPQ and total PARP. Representative image of 3 biological replicates (with two technical replicates) is shown. (**E**) Western blot validation of HA-CK1α ectopic expression in SFPQ-depleted HCT-116 cells. β-tubulin was used as loading control. Representative of three biological replicates is shown. (**F**) HA-CK1α ectopic expression rescues growth of SFPQ-depleted HCT-116 cells. Western blot validation of protein expression can be found in Supplementary Figure S5. Empty vector is used as control for HA-CK1α and siCtrl is used as control for the siSFPQ constructs. Either wild-type (WT) or kinase-dead (KD) HA-CK1α is expressed alongside treatment with siSFPQ #6 or #9. Each assay was performed in quadruplicates and repeated in three independent experiments, n = 3, $N = 12$. All individual data points represent values from independent experiments (with mean ± SD).

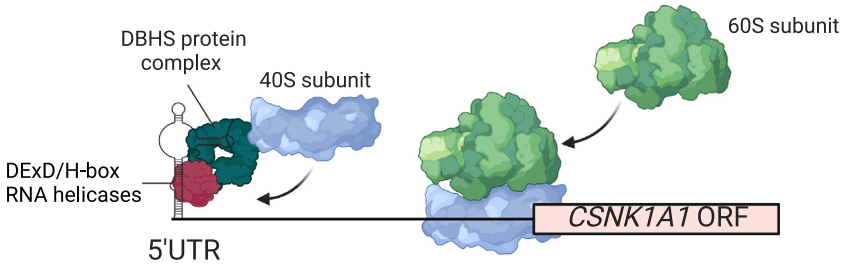

Figure 6. Proposed working model of IRES-mediated CK1α translation by 5′-UTR-associated RBPs in RAS-mutant cancer cells. Binding of translation complexes, involving DBHS proteins (SFPQ, PSCP1, NONO) and/or other RBPs (DExD/H-box RNA helicases, etc) (79,80), to the CK1α 5′-UTR may allow direct recruitment of 40S ribosomal subunit to the CK1α mRNA in RAS-mutant cancer cells. The 40S ribosomal subunit scans along the 5′-UTR until it arrives at the start codon of the CK1α transcript, where subsequent recruitment of the 60S ribosomal subunit occurs to promote translation initiation of CK1α. Illustration created with BioRender.com.

CK1α 5′-UTR (Figure 3D, Supplementary Table S7). These DBHS proteins are known to function as obligate dimers (68–71), but it remains unknown whether different DBHS heterodimers differentially regulate CK1α expression in RAS-mutant cancer cells. Using orthogonal assays like RNA-IP, we confirmed that SFPQ directly binds to the CK1α 5′-UTR and further showed that both RNA recognition motifs of SFPQ (RRM1 and RRM2) are required for this interaction (Figure 3F).

Importantly, we found SFPQ, DDX6 and other CK1α 5′-UTR-associated RBPs to be upregulated in a number of human cancers that are often associated with KRAS-activating mutations (Figure 4A–F, Supplementary Figure S4A–C). We further showed that the protein abundance of these CK1α 5′-UTR-associated RBPs are significantly elevated in a mutant RAS-specific manner (Figure 4A, B). Consistent with our previous observation that inhibition of CK1α blocked HCT-116 colon cancer cell growth (11), siRNA depletion of SFPQ induced downregulation of CK1α protein expression and partial blockade of HCT-116 colon cancer cell growth (Figure 5A, E, F), indicating that SFPQ is a tractable target for RAS-mutant cancers. Our findings also corroborate past literature that reported various roles of SFPQ in promoting tumor progression, including regulation of DNA damage response (72), clonogenic survival and radio-resistance (73). For instance, upregulation of SFPQ promotes the expression of specific oncogenic transcripts, such as *SOX10*, *AMIGO2* and *LINC00511*, in BRAF-mutant melanoma cancer cells (74). Notably, loss of SFPQ induces R-loop (DNA-RNA hybrid) formation to confer DNA replicative stress and trigger apoptosis in BRAF-mutant colorectal cancer cells (75). Elevated SFPQ has also been shown to enhance the expression of spliceosome genes and promote androgen receptor (AR) splicing in advanced or metastatic prostate cancer cells (45). Furthermore, AR-induced long non-coding RNA *LINC01503* recruits SFPQ to activate FOSL1 transcription to promote nasopharyngeal carcinoma cell proliferation and metastasis (76). Similarly, SFPQ augments the expression and nuclear export of *ESR1*, *SCFD2*, *TRA2B* and *ASPM* mRNAs to drive ER-positive breast cancer progression (77).

The data led us to propose a working model in which DBHS proteins (SFPQ, etc) (78) and/or other CK1α 5′-UTR associated RBPs (DExD/H-box RNA helicases, etc) collectively govern CK1α oncoprotein expression and the growth/survival of RAS-mutant cancers (Figure 6). This is consistent with reports that showed interactions of DBHS proteins with DExD/H-box RNA helicases and 40S ribosomes, respectively, to control protein expression (79,80), and underscores a critical role of complex RBP-RNA networks in promoting tumorigenesis and/or cancer progression (81,82).

In conclusion, our study identifies SFPQ and several other RBPs that interact with the 5′-UTR of CK1α to modulate protein expression of this oncogenic kinase in RAS-mutant cancer cells. Intriguingly, the expression of these RBPs are also regulated in a mutant RAS-specific manner. Our ongoing research effort, therefore, seeks to elucidate the mechanism by which mutant KRAS controls expression of these identified RBPs to alter cell fate via dramatic translation remodelling of the proteome. The ability to target these RBPs in RAS-mutant cancers using nucleotide-based agents (e.g. antisense oligonucleotides and siRNAs) and/or small molecules (83) may present a novel approach to treat this common subset of cancers.

CONSENT FOR PUBLICATION

The authors have approved the manuscript for publication.

DATA AVAILABILITY

Data supporting the conclusions of this study are included within the article and its additional files. The mass spectrometry proteomics data are available via Proteomics IDEntifications database, PRIDE, with identifier PXD027124.

SUPPLEMENTARY DATA

Supplementary Data are available at NAR Cancer Online.

ACKNOWLEDGEMENTS

We are greatly indebted to David Virshup (Duke-NUS) and Heng-Phon Too (NUS) for reagents, helpful discussions and critical review of this work. We also thank Kuo-Chieh Liao (GIS) for reagents and our lab intern Hongyi Le (Hwa Chong International School) for his assistance in performing part of the Oncomine analysis, which was regrettably excluded in this manuscript.

Author contributions: J.J.E.C. and J.K.C. conceived the project and designed the experiments. V.J.T.K., J.J.E.C. and J.K.C. analyzed the publicly available cancer genome/proteome databases. V.J.T.K., J.Y.T., S.Y.T., C.H.Q., W.X.L., J.T.F.C., G.W.L.E., T.K.L. and J.K.C. performed experiments and analyzed data. Q.S.L., J.J.E.C. and J.K.C. supervised experiments and interpreted experimental data. V.J.T.K., J.J.E.C. and J.K.C. wrote the paper. All authors discussed the results and commented on the manuscript.

FUNDING

GWLE is supported by the Singapore Ministry of Education Postdoctoral Fellowship at the National University of Singapore. JKC is supported by the Singapore MOE AcRF Tier 2 grant (MOE2016-T2-2-052) and a start-up grant from Yong Loo Lin School of Medicine, National University of Singapore.
Conflict of interest statement. None declared.

REFERENCES

1. Prior,I.A., Lewis,P.D. and Mattos,C. (2012) A comprehensive survey of Ras mutations in cancer. *Cancer Res.*, **72**, 2457.
2. Stephen,A.G., Esposito,D., Bagni,R.K. and McCormick,F. (2014) Dragging Ras back in the ring. *Cancer Cell*, **25**, 272–281.
3. Vaughn,C.P., ZoBell,S.D., Furtado,L.V., Baker,C.L. and Samowitz,W.S. (2011) Frequency of KRAS, BRAF, and NRAS mutations in colorectal cancer. *Genes Chromosomes Cancer*, **50**, 307–312.
4. Al-Mulla,F., Milner-White,E.J., Going,J.J. and Birnie,G.D. (1999) Structural differences between valine-12 and aspartate-12 Ras proteins may modify carcinoma aggression. *J. Pathol.*, **187**, 433–438.
5. Smith,G., Bounds,R., Wolf,H., Steele,R.J.C., Carey,F.A. and Wolf,C.R. (2010) Activating K-Ras mutations outwith 'hotspot' codons in sporadic colorectal tumours - implications for personalised cancer medicine. *Br. J. Cancer*, **102**, 693–703.
6. Tejpar,S., Celik,I., Schlichting,M., Sartorius,U., Bokemeyer,C. and Van Cutsem,E. (2012) Association of KRAS G13D tumor mutations with outcome in patients with metastatic colorectal cancer treated with first-line chemotherapy with or without cetuximab. *J. Clin. Oncol.*, **30**, 3570–3577.
7. Osumi,H., Shinozaki,E., Osako,M., Kawazoe,Y., Oba,M., Misaka,T., Goto,T., Kamo,H., Suenaga,M., Kumekawa,Y. *et al.* (2015) Cetuximab treatment for metastatic colorectal cancer with KRAS p.G13D mutations improves progression-free survival. *Mol. Clin. Oncol.*, **3**, 1053–1057.
8. Cox,A.D., Fesik,S.W., Kimmelman,A.C., Luo,J. and Der,C.J. (2014) Drugging the undruggable RAS: Mission Possible?*Nat. Rev. Drug Discov.*, **13**, 828–851.
9. Stalnecker,C.A. and Der,C.J. (2020) RAS, wanted dead or alive: Advances in targeting RAS mutant cancers. *Sci. Signal*, **13**, eaay6013.
10. Atefi,M., Titz,B., Avramis,E., Ng,C., Wong,D.J.L., Lassen,A., Cerniglia,M., Escuin-Ordinas,H., Foulad,D., Comin-Anduix,B. *et al.* (2015) Combination of pan-RAF and MEK inhibitors in NRAS mutant melanoma. *Mol. Cancer*, **14**, 27.
11. Cheong,J.K., Zhang,F., Chua,P.J., Bay,B.H., Thorburn,A. and Virshup,D.M. (2015) Casein kinase 1α-dependent feedback loop controls autophagy in RAS-driven cancers. *J. Clin. Invest.*, **125**, 1401–1418.
12. Jiang,S., Zhang,M., Sun,J. and Yang,X. (2018) Casein kinase 1α: biological mechanisms and theranostic potential. *Cell Commun. Signal.*, **16**, 23.
13. Schuster,S.L. and Hsieh,A.C. (2019) the Untranslated Regions of mRNAs in Cancer. *Trends Cancer*, **5**, 245–262.
14. Cenik,C., Chua,H.N., Zhang,H., Tarnawsky,S.P., Akef,A., Derti,A., Tasan,M., Moore,M.J., Palazzo,A.F. and Roth,F.P. (2011) Genome analysis reveals interplay between 5′UTR introns and nuclear mRNA export for secretory and mitochondrial genes. *PLoS Genet.*, **7**, e1001366.
15. Weinhold,N., Jacobsen,A., Schultz,N., Sander,C. and Lee,W. (2014) Genome-wide analysis of noncoding regulatory mutations in cancer. *Nat. Genet.*, **46**, 1160–1165.
16. Marques-Ramos,A., Candeias,M.M., Menezes,J., Lacerda,R., Willcocks,M., Teixeira,A., Locker,N. and Romão,L. (2017) Cap-independent translation ensures mTOR expression and function upon protein synthesis inhibition. *RNA*, **23**, 1712–1728.
17. Chua,J.J.E., Schob,C., Rehbein,M., Gkogkas,C.G., Richter,D. and Kindler,S. (2012) Synthesis of two SAPAP3 isoforms from a single mRNA is mediated via alternative translational initiation. *Sci. Rep.*, **2**, 484–484.
18. Ward,A.M., Bidet,K., Yinglin,A., Ler,S.G., Hogue,K., Blackstock,W., Gunaratne,J. and Garcia-Blanco,M.A. (2011) Quantitative mass spectrometry of DENV-2 RNA-interacting proteins reveals that the DEAD-box RNA helicase DDX6 binds the DB1 and DB2 3′ UTR structures. *RNA Biol*, **8**, 1173–1186.
19. Ren,F., Zhu,J., Li,K., Cheng,Y. and Zhu,X. (2020) CK1α-targeting inhibits primary and metastatic colorectal cancer in vitro, ex vivo, in cell-line-derived and patient-derived tumor xenograft mice models. *Transl. Cancer Res.*, **9**, 1903–1913.
20. Cai,J., Li,R., Xu,X., Zhang,L., Lian,R., Fang,L., Huang,Y., Feng,X., Liu,X., Li,X. *et al.* (2018) CK1α suppresses lung tumour growth by stabilizing PTEN and inducing autophagy. *Nat. Cell Biol.*, **20**, 465–478.
21. Leppek,K., Das,R. and Barna,M. (2018) Functional 5′ UTR mRNA structures in eukaryotic translation regulation and how to find them. *Nat. Rev. Mol. Cell Biol.*, **19**, 158–174.
22. Pesole,G., Mignone,F., Gissi,C., Grillo,G., Licciulli,F. and Liuni,S. (2001) Structural and functional features of eukaryotic mRNA untranslated regions. *Gene*, **276**, 73–81.
23. Chappell,S.A., Edelman,G.M. and Mauro,V.P. (2000) a 9-nt segment of a cellular mRNA can function as an internal ribosome entry site (IRES) and when present in linked multiple copies greatly enhances IRES activity. *Proc. Natl. Acad. Sci. U.S.A.*, **97**, 1536–1541.
24. Jimenez,J., Jang,G.M., Semler,B.L. and Waterman,M.L. (2005) an internal ribosome entry site mediates translation of lymphoid enhancer factor-1. *RNA*, **11**, 1385–1399.
25. Rubtsova,M.P., Sizova,D.V., Dmitriev,S.E., Ivanov,D.S., Prassolov,V.S. and Shatsky,I.N. (2003) Distinctive properties of the 5′-untranslated region of human Hsp70 mRNA. *J. Biol. Chem.*, **278**, 22350–22356.
26. Babendure,J.R., Babendure,J.L., Ding,J.-H. and Tsien,R.Y. (2006) Control of mammalian translation by mRNA structure near caps. *RNA*, **12**, 851–861.
27. Zuker,M. (2003) Mfold web server for nucleic acid folding and hybridization prediction. *Nucleic Acids Res.*, **31**, 3406–3415.
28. Baird,S.D., Turcotte,M., Korneluk,R.G. and Holcik,M. (2006) Searching for IRES. *RNA*, **12**, 1755–1785.
29. Candeias,M.M., Powell,D.J., Roubalova,E., Apcher,S., Bourougaa,K., Vojtesek,B., Bruzzoni-Giovanelli,H. and Fåhraeus,R. (2006) Expression of p53 and p53/47 are controlled by alternative mechanisms of messenger RNA translation initiation. *Oncogene*, **25**, 6936–6947.
30. Damiano,F., Alemanno,S., Gnoni,G.V. and Siculella,L. (2010) Translational control of the sterol-regulatory transcription factor SREBP-1 mRNA in response to serum starvation or ER stress is mediated by an internal ribosome entry site. *Biochem. J.*, **429**, 603–612.
31. King,H.A., Cobbold,L.C. and Willis,A.E. (2010) the role of IRES trans-acting factors in regulating translation initiation. *Biochem. Soc. Trans.*, **38**, 1581–1586.
32. Mellacheruvu,D., Wright,Z., Couzens,A.L., Lambert,J.P., St-Denis,N.A., Li,T., Miteva,Y.V., Hauri,S., Sardiu,M.E., Low,T.Y. *et al.* (2013) the CRAPome: a contaminant repository for affinity purification-mass spectrometry data. *Nat. Methods*, **10**, 730–736.
33. Muppirala,U.K., Honavar,V.G. and Dobbs,D. (2011) Predicting RNA-protein interactions using only sequence information. *BMC Bioinf.*, **12**, 489.
34. Klotz-Noack,K., Klinger,B., Rivera,M., Bublitz,N., Uhlitz,F., Riemer,P., Lüthen,M., Sell,T., Kasack,K., Gastl,B. *et al.* (2020) SFPQ depletion is synthetically lethal with BRAF(V600E) in colorectal cancer cells. *Cell Rep.*, **32**, 108184.

35. Yeh,H.W., Hsu,E.C., Lee,S.S., Lang,Y.D., Lin,Y.C., Chang,C.Y., Lee,S.Y., Gu,D.L., Shih,J.H., Ho,C.M. *et al.* (2018) PSPC1 mediates TGF-β1 autocrine signalling and Smad2/3 target switching to promote EMT, stemness and metastasis. *Nat. Cell Biol.*, **20**, 479–491.
36. Yin,X.-K., Wang,Y.-L., Wang,F., Feng,W.-X., Bai,S.-M., Zhao,W.-W., Feng,L.-L., Wei,M.-B., Qin,C.-L., Wang,F. *et al.* (2021) PRMT1 enhances oncogenic arginine methylation of NONO in colorectal cancer. *Oncogene*, **40**, 1375–1389.
37. Kim,C.Y., Jung,W.Y., Lee,H.J., Kim,H.K., Kim,A. and Shin,B.K. (2012) Proteomic analysis reveals overexpression of moesin and cytokeratin 17 proteins in colorectal carcinoma. *Oncol. Rep.*, **27**, 608–620.
38. Taniguchi,K., Sugito,N., Kumazaki,M., Shinohara,H., Yamada,N., Matsuhashi,N., Futamura,M., Ito,Y., Otsuki,Y., Yoshida,K. *et al.* (2015) Positive feedback of DDX6/c-Myc/PTB1 regulated by miR-124 contributes to maintenance of the Warburg effect in colon cancer cells. *Biochim. Biophys. Acta Mol. Basis Dis.*, **1852**, 1971–1980.
39. Chen,S., Zhang,J., Duan,L., Zhang,Y., Li,C., Liu,D., Ouyang,C., Lu,F. and Liu,X. (2013) Identification of HnRNP M as a novel biomarker for colorectal carcinoma by quantitative proteomics. *Am. J. Physiol.-Gastrointestinal Liver Physiol.*, **306**, G394–G403.
40. Park,S., Brugiolo,M., Akerman,M., Das,S., Urbanski,L., Geier,A., Kesarwani,A.K., Fan,M., Leclair,N., Lin,K.-T. *et al.* (2019) Differential functions of splicing factors in mammary transformation and breast cancer metastasis. *Cell Rep.*, **29**, 2672–2688.
41. Iino,K., Mitobe,Y., Ikeda,K., Takayama,K.-I., Suzuki,T., Kawabata,H., Suzuki,Y., Horie-Inoue,K. and Inoue,S. (2020) RNA-binding protein NONO promotes breast cancer proliferation by post-transcriptional regulation of SKP2 and E2F8. *Cancer Sci.*, **111**, 148–159.
42. Lang,Y.-D., Chen,H.-Y., Ho,C.-M., Shih,J.-H., Hsu,E.-C., Shen,R., Lee,Y.-C., Chen,J.-W., Wu,C.-Y., Yeh,H.-W. *et al.* (2019) PSPC1-interchanged interactions with PTK6 and β-catenin synergize oncogenic subcellular translocations and tumor progression. *Nat. Commun.*, **10**, 5716.
43. Kim,S.-J., Ju,J.-S., Kang,M.-H., Won,J.E., Kim,Y.H., Raninga,P.V., Khanna,K.K., Győrffy,B., Pack,C.-G., Han,H.-D. *et al.* (2020) RNA-binding protein NONO contributes to cancer cell growth and confers drug resistance as a theranostic target in TNBC. *Theranostics*, **10**, 7974–7992.
44. Mura,M., Hopkins,T.G., Michael,T., Abd-Latip,N., Weir,J., Aboagye,E., Mauri,F., Jameson,C., Sturge,J., Gabra,H. *et al.* (2015) LARP1 post-transcriptionally regulates mTOR and contributes to cancer progression. *Oncogene*, **34**, 5025–5036.
45. Takayama,K.-i., Suzuki,T., Fujimura,T., Yamada,Y., Takahashi,S., Homma,Y., Suzuki,Y. and Inoue,S. (2017) Dysregulation of spliceosome gene expression in advanced prostate cancer by RNA-binding protein PSF. *Proc. Natl. Acad. Sci. U.S.A.*, **114**, 10461.
46. Rebay,I., Chen,F., Hsiao,F., Kolodziej,P.A., Kuang,B.H., Laverty,T., Suh,C., Voas,M., Williams,A. and Rubin,G.M. (2000) A genetic screen for novel components of the Ras/mitogen-activated protein kinase signaling pathway that interact with the *yan* gene of Drosophila identifies *split ends*, a new RNA recognition motif-containing protein. *Genetics*, **154**, 695.
47. Moore,A.R., Rosenberg,S.C., McCormick,F. and Malek,S. (2020) RAS-targeted therapies: is the undruggable drugged?*Nat. Rev. Drug Discov.*, **19**, 533–552.
48. Chang,K., Creighton,C.J., Davis,C., Donehower,L., Drummond,J., Wheeler,D., Ally,A., Balasundaram,M., Birol,I., Butterfield,Y.S.N. *et al.* (2013) The Cancer Genome Atlas Pan-Cancer analysis project. *Nat. Genet.*, **45**, 1113–1120.
49. Tang,Z., Li,C., Kang,B., Gao,G., Li,C. and Zhang,Z. (2017) GEPIA: a web server for cancer and normal gene expression profiling and interactive analyses. *Nucleic Acids Res.*, **45**, W98–W102.
50. Chen,F., Chandrashekar,D.S., Varambally,S. and Creighton,C.J. (2019) Pan-cancer molecular subtypes revealed by mass-spectrometry-based proteomic characterization of more than 500 human cancers. *Nat. Commun.*, **10**, 5679.
51. Chandrashekar,D.S., Bashel,B., Balasubramanya,S.A.H., Creighton,C.J., Ponce-Rodriguez,I., Chakravarthi,B.V.S.K. and Varambally,S. (2017) UALCAN: a portal for facilitating tumor subgroup gene expression and survival analyses. *Neoplasia*, **19**, 649–658.
52. Cheong,J.K. and Virshup,D.M. (2011) Casein kinase 1: complexity in the family. *Int. J. Biochem. Cell Biol.*, **43**, 465–469.
53. Zhang,F., Virshup,D.M. and Cheong,J.K. (2018) Oncogenic RAS-induced CK1α drives nuclear FOXO proteolysis. *Oncogene*, **37**, 363–376.
54. Liu,X., Huang,Q., Chen,L., Zhang,H., Schonbrunn,E. and Chen,J. (2020) Tumor-derived CK1α mutations enhance MDMX inhibition of p53. *Oncogene*, **39**, 176–186.
55. Zhang,P., Bill,K., Liu,J., Young,E., Peng,T., Bolshakov,S., Hoffman,A., Song,Y., Demicco,E.G., Terrada,D.L. *et al.* (2012) MiR-155 is a liposarcoma oncogene that targets casein kinase-1α and enhances β-catenin signaling. *Cancer Res.*, **72**, 1751–1762.
56. Davuluri,R.V., Suzuki,Y., Sugano,S. and Zhang,M.Q. (2000) CART classification of human 5′ UTR sequences. *Genome Res.*, **10**, 1807–1816.
57. Sriram,A., Bohlen,J. and Teleman,A.A. (2018) Translation acrobatics: how cancer cells exploit alternate modes of translational initiation. *EMBO Rep.*, **19**, e45947.
58. Holmes,B., Lee,J., Landon,K.A., Benavides-Serrato,A., Bashir,T., Jung,M.E., Lichtenstein,A. and Gera,J. (2016) Mechanistic target of rapamycin (mTOR) inhibition synergizes with reduced internal ribosome entry site (IRES)-mediated translation of cyclin D1 and c-MYC mRNAs to treat glioblastoma. *J. Biol. Chem.*, **291**, 14146–14159.
59. Wang,H., Zhu,Y., Hu,L., Li,Y., Liu,G., Xia,T., Xiong,D., Luo,Y., Liu,B., An,Y. *et al.* (2020) Internal ribosome entry sites mediate Cap-independent translation of Bmi1 in nasopharyngeal carcinoma. *Front. Oncol.*, **10**, 1678.
60. Spriggs,K.A., Bushell,M. and Willis,A.E. (2010) Translational Regulation of Gene Expression during Conditions of Cell Stress. *Mol. Cell*, **40**, 228–237.
61. Wolfe,A.L., Singh,K., Zhong,Y., Drewe,P., Rajasekhar,V.K., Sanghvi,V.R., Mavrakis,K.J., Jiang,M., Roderick,J.E., Van der Meulen,J. *et al.* (2014) RNA G-quadruplexes cause eIF4A-dependent oncogene translation in cancer. *Nature*, **513**, 65–70.
62. Liu,Y., Horn,J.L., Banda,K., Goodman,A.Z., Lim,Y., Jana,S., Arora,S., Germanos,A.A., Wen,L., Hardin,W.R. *et al.* (2019) the androgen receptor regulates a druggable translational regulon in advanced prostate cancer. *Sci. Transl. Med.*, **11**, eaaw4993.
63. Blazie,S.M., Takayanagi-Kiya,S., McCulloch,K.A. and Jin,Y. (2021) Eukaryotic initiation factor EIF-3.G augments mRNA translation efficiency to regulate neuronal activity. *Elife*, **10**, e68336.
64. Choe,J., Oh,N., Park,S., Lee,Y.K., Song,O.K., Locker,N., Chi,S.G. and Kim,Y.K. (2012) Translation initiation on mRNAs bound by nuclear cap-binding protein complex CBP80/20 requires interaction between CBP80/20-dependent translation initiation factor and eukaryotic translation initiation factor 3g. *J. Biol. Chem.*, **287**, 18500–18509.
65. Yang,Y. and Wang,Z. (2019) IRES-mediated cap-independent translation, a path leading to hidden proteome. *J. Mol. Cell Biol.*, **11**, 911–919.
66. Stripecke,R., Oliveira,C.C., McCarthy,J.E. and Hentze,M.W. (1994) Proteins binding to 5′ untranslated region sites: a general mechanism for translational regulation of mRNAs in human and yeast cells. *Mol. Cell. Biol.*, **14**, 5898–5909.
67. Kechavarzi,B. and Janga,S.C. (2014) Dissecting the expression landscape of RNA-binding proteins in human cancers. *Genome Biol.*, **15**, R14.
68. Dong,B., Horowitz,D.S., Kobayashi,R. and Krainer,A.R. (1993) Purification and cDNA cloning of HeLa cell p54nrb, a nuclear protein with two RNA recognition motifs and extensive homology to human splicing factor PSF and Drosophila NONA/BJ6. *Nucleic Acids Res.*, **21**, 4085–4092.
69. Lee,M., Sadowska,A., Bekere,I., Ho,D., Gully,B.S., Lu,Y., Iyer,K.S., Trewhella,J., Fox,A.H. and Bond,C.S. (2015) the structure of human SFPQ reveals a coiled-coil mediated polymer essential for functional aggregation in gene regulation. *Nucleic Acids Res.*, **43**, 3826–3840.
70. Li,S., Kuhne,W.W., Kulharya,A., Hudson,F.Z., Ha,K., Cao,Z. and Dynan,W.S. (2009) Involvement of p54(nrb), a PSF partner protein, in DNA double-strand break repair and radioresistance. *Nucleic Acids Res.*, **37**, 6746–6753.
71. Knott,G.J., Bond,C.S. and Fox,A.H. (2016) the DBHS proteins SFPQ, NONO and PSPC1: a multipurpose molecular scaffold. *Nucleic Acids Res.*, **44**, 3989–4004.

72. Rajesh,C., Baker,D.K., Pierce,A.J. and Pittman,D.L. (2011) the splicing-factor related protein SFPQ/PSF interacts with RAD51D and is necessary for homology-directed repair and sister chromatid cohesion. *Nucleic Acids Res.*, **39**, 132–145.
73. Ha,K., Takeda,Y. and Dynan,W.S. (2011) Sequences in PSF/SFPQ mediate radioresistance and recruitment of PSF/SFPQ-containing complexes to DNA damage sites in human cells. *DNA Repair (Amst.)*, **10**, 252–259.
74. Bi,O., Anene,C.A., Nsengimana,J., Shelton,M., Roberts,W., Newton-Bishop,J. and Boyne,J.R. (2021) SFPQ promotes an oncogenic transcriptomic state in melanoma. *Oncogene*, **40**, 5192–5203.
75. Klotz-Noack,K., Klinger,B., Rivera,M., Bublitz,N., Uhlitz,F., Riemer,P., Lüthen,M., Sell,T., Kasack,K., Gastl,B. *et al.* (2020) SFPQ depletion is synthetically lethal with $BRAF^{V600E}$ in colorectal cancer cells. *Cell Rep.*, **32**, 108184.
76. He,S.-W., Xu,C., Li,Y.-Q., Li,Y.-Q., Zhao,Y., Zhang,P.-P., Lei,Y., Liang,Y.-L., Li,J.-Y., Li,Q. *et al.* (2020) AR-induced long non-coding RNA LINC01503 facilitates proliferation and metastasis via the SFPQ-FOSL1 axis in nasopharyngeal carcinoma. *Oncogene*, **39**, 5616–5632.
77. Mitobe,Y., Iino,K., Takayama,K.-i., Ikeda,K., Suzuki,T., Aogi,K., Kawabata,H., Suzuki,Y., Horie-Inoue,K. and Inoue,S. (2020) PSF promotes ER-positive breast cancer progression via posttranscriptional regulation of *ESR1* and *SCFD2*. *Cancer Res.*, **80**, 2230.
78. Zhou,B., Wu,F., Han,J., Qi,F., Ni,T. and Qian,F. (2019) Exploitation of nuclear protein SFPQ by the encephalomyocarditis virus to facilitate its replication. *Biochem. Biophys. Res. Commun.*, **510**, 65–71.
79. Wang,J., Rajbhandari,P., Damianov,A., Han,A., Sallam,T., Waki,H., Villanueva,C.J., Lee,S.D., Nielsen,R., Mandrup,S. *et al.* (2017) RNA-binding protein PSPC1 promotes the differentiation-dependent nuclear export of adipocyte RNAs. *J. Clin. Invest.*, **127**, 987–1004.
80. Chakraborty,P., Huang,J.T.J. and Hiom,K. (2018) DHX9 helicase promotes R-loop formation in cells with impaired RNA splicing. *Nat. Commun.*, **9**, 4346.
81. Pereira,B., Billaud,M. and Almeida,R. (2017) RNA-binding proteins in cancer: old players and new actors. *Trends Cancer*, **3**, 506–528.
82. Qin,H., Ni,H., Liu,Y., Yuan,Y., Xi,T., Li,X. and Zheng,L. (2020) RNA-binding proteins in tumor progression. *J. Hematol. Oncol.*, **13**, 90.
83. Wu,P. (2020) Inhibition of RNA-binding proteins with small molecules. *Nat. Rev. Chem.*, **4**, 441–458.